Corrosion of Sintered NdFeB Permanent Magnets

View the article online for updates and enhancements.

Corrosion of Sintered NdFeB Permanent Magnets

Terezija Poženel Kovačič,[1] **Nataša Kovačević,**[2] and **Ingrid Milošev**[1,*,z]

[1]*Jožef Stefan Institute, Department of Physical and Organic Chemistry, SI-1000 Ljubljana, Slovenia*
[2]*Kolektor Mobility d.o.o., SI-5280 Idrija, Slovenia*

The green transition to reduce reliance on fossil fuel energy sources and minimise global warming is accelerating the need for NdFeB permanent magnet materials. Sintered NdFeB magnets cover the largest segment percentage within the permanent magnet type group, with a share of over 50%. The microstructure of NdFeB magnets includes grains of the $Nd_{1+\varepsilon}Fe_4B_4$ (B-rich phase), which form grain boundaries with both the Nd-rich (Nd_4Fe) and matrix ($Nd_2Fe_{14}B$) phases. NdFeB magnets are prone to degradation in harsh environments due to the low corrosion resistance of both iron and neodymium. Consequently, magnets require corrosion protection because their magnetic properties would be jeopardised due to the degradation caused by the corrosion process. Understanding magnets' electrochemical and corrosion properties is crucial for developing their corrosion protection and thus prolonging their smooth operation in numerous industrial applications. This review aims to present the fundamental corrosion processes on sintered NdFeB magnets, provide an overview of the contemporary magnet production processes of NdFeB magnets and their impact on the corrosion resistance, and summarise the corrosion protection of NdFeB magnets. Prospects are presented, especially regarding the use of magnets in the transportation (hybrid and electric vehicles) industry and the development of alternative types of coatings.

Since the first announcement of the body-centred tetragonal $Nd_2Fe_{14}B$ phase as a new magnet material in the 1980s, it has continued to gain importance. Neodymium–iron–boron (NdFeB) magnets were independently prepared by two technologies and two research groups. In 1984, Sagawa et al. employed the powder metallurgy technique (sintering),[1] and Croat et al. used the melt-spinning technique.[2] From that point on, sintered NdFeB permanent magnets have played an important role in the technical development of different industries and applications, including electronics and consumer electronics, household appliances, industrial automation equipment, medical devices, aerospace and defence industry, electric power generation and conversion, including renewable energy technologies like wind power.[3] Neodymium magnets also play an essential role in the automotive industry. Relatively rapid transformation from internal combustion engine vehicles (ICEV) to electric vehicles (EV) also requires a steep change in the demand for and supply of the raw materials used in the production process. Overall, NdFeB magnets are inevitable in modern technology and are found in numerous products and systems we encounter daily.[4–7]

Magnetisation (M) is the key quantity in ferromagnets such as sintered NdFeB magnets. Ferromagnetism is a property of certain materials (such as iron) that allows them to exhibit strong, permanent magnetic behaviour. It arises from the alignment of magnetic moments (small magnetic fields produced by atoms) in the material. This alignment results in a significant, observable magnetic permeability and, in many cases, a significant magnetic coercivity, allowing the material to form a permanent magnet. According to the coercivity (H_c), defined as the magnet resistance against demagnetisation (as will be discussed below), magnetic materials can be classified into three groups: soft ($H_c < 1$ kA m^{-1}), hard ($H_c > 100$ kA m^{-1}), and semi-hard (1 kA m^{-1} $< H_c < 100$ kA m^{-1}) (Fig. 1). This review is focused on sintered NdFeB magnets, which belong to hard magnetic materials, along with samarium–cobalt (Sm–Co) and ferrite (α-iron(III) oxide-containing magnetic materials). Sintered magnets produced at high temperatures (about 1100 °C) have the highest magnetic properties, whereas magnets produced by bonding magnetic powder with a polymer binder, such as polyamides or polyphenylene sulphide, exhibit lower magnetic properties.[4,8–10]

Among hard magnetic materials, ferrites and Alnicos were first developed. Ferrites are a class of ceramic materials made from iron oxide mixed with other metal oxides (e.g., manganese, zinc, or nickel). They are magnetically active materials, but are not always used as permanent magnets. Alnico materials are a family of iron-based alloys known for their strong magnetic properties. The name "Alnico" is derived from the primary elements that make up the alloy: aluminium (Al), nickel (Ni), and cobalt (Co). Other elements, such as iron (Fe), copper (Cu), and titanium (Ti), are also included in varying amounts to enhance specific properties. In the early 1960s, samarium–cobalt (Sm–Co) magnets were developed. They are rare-earth permanent magnets ranked similarly in strength to neodymium magnets but have higher temperature ratings and coercivity. Finally, NdFeB magnets emerged in the 1980s and soon became the most widely used rare-earth magnets.[11]

Sintered NdFeB magnet covers the largest segment percentage within the permanent magnet type group, with a share of over 50% (Fig. 2a). The second largest share is related to sintered ferrite, followed by bonded ferrite and bonded NdFeB. The political decisions to move forward with the green transition to reduce reliance on fossil fuel energy sources and minimise global warming are accelerating the need for NdFeB permanent magnet materials. According to the growth factors, market dynamics and competitive analysis, the permanent magnet market is anticipated to expand further during the forecast period of 2024–2031.[12] The largest share according to the type of applications is in motors and generators (Fig. 2b), where NdFeB magnets are used in the electric motors, which are responsible for the vehicle's propulsion, as well as magnetic brakes, bearings, etc. Sintered NdFeB magnets bring significant benefits to electric vehicles. Their superior magnetic properties enable electric motors to achieve a high torque-to-weight ratio, enhancing vehicle performance and acceleration. Moreover, their compact design facilitates the creation of smaller, lighter motors, contributing to more streamlined and efficient vehicle designs. These magnets also excel in heat resistance, making them ideal for the challenging conditions within electric vehicle motors.[13] Their ability to operate effectively at relatively high temperatures ensures consistent motor efficiency and reduces the likelihood of component failures.

The following largest share is in electronic products, namely hard disk drives (HDDs), compact discs (CDs) and digital video discs (DVDs), where data storage is based on magnetism (Fig. 2b).[16] Large shares of magnet applications belong to transportation (such
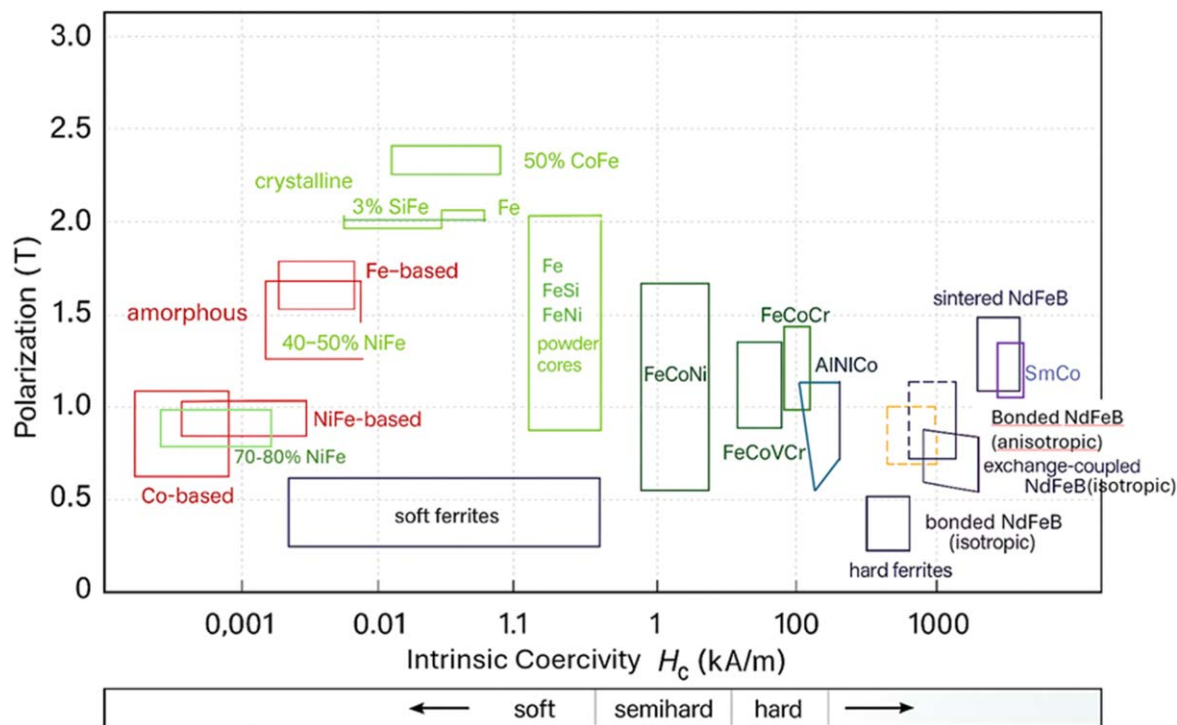
Figure 1. Polarisation vs coercivity of soft and hard magnetic materials.[4] *Reprinted with permission from the WILEY-VCH Verlag GmbH.*
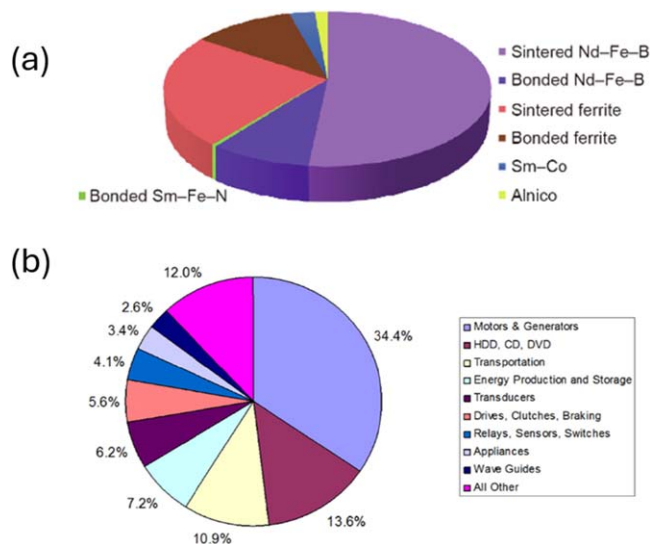

Figure 2. (a) Market shares of various types of magnets and (b) applications where permanent NdFeB magnet materials are used.[14,15] *Reprinted with permission from the Higher Education Press Limited Company (Chinese Academy of Engineering).*

as magnetic suspension trains, window opening motors and door locks), energy production and storage, appliances, etc.

Due to the large worldwide demand for permanent magnets and the significant reductions in China's export quotas, in 2010/2011, a Rare Earth Crisis initiated a quest for permanent magnets without or with reduced amounts of critical rare earth metals. Still, today, China covers at least 80% of the world's supply of rare earth metals. Not only does a major part of the extraction of heavy rare earths take place in China, but it also has the majority of supply chains for converting raw elements into end products under its control. Alternative sources of supply are under development in Australia, Canada, Brazil, South Africa, Vietnam and Sweden, but this is a

long-term and risky investment in mines, which usually raises opposition from environmentalists.

NdFeB magnets are prone to degradation in harsh environments due to the low corrosion resistance of both iron and neodymium. Consequently, magnets require corrosion protection since their magnetic properties would be jeopardised due to the degradation caused by the corrosion process. As the significance of these magnets continues to grow, we identified the need for a systematic approach to organising and consolidating existing knowledge about their corrosion behaviour, specifically of sintered NdFeB permanent magnets, representing the largest market share. The structure of this review is as follows. First, the general properties of the NdFeB magnets are described, followed by the presentation of fundamental corrosion processes in various solutions (aqueous, non-aqueous and vapour). Second, contemporary approaches to magnet production processes aiming to improve magnetic behaviour and corrosion resistance through changes in their microstructure are presented. Third, state-of-the-art corrosion protection by modification of the magnets' surface by protective coatings is summarised.

Magnetic Properties, Composition and Microstructure of Sintered NdFeB Permanent Magnets

Sintered NdFeB permanent magnet contains the essential rare earth element (REE) of neodymium. Nd atoms, coupling with ferromagnetic element Fe atoms, help the magnet obtain high remanence (B_r), which is the residual magnetisation in the absence of an external magnetic field, and maximum energy product ($(BH)_{max}$), (Fig. 3). Permanent magnet energy product $(BH)_{max}$ is an important parameter representing the maximum energy per unit volume that a magnet can deliver in a system. Another critical parameter is high coercivity (H_{cj}), which is the magnet's resistance against demagnetisation. A hysteresis curve, also known as a magnetisation curve or *B–H* curve, graphically represents the relationships mentioned above and provides valuable insights into the magnetic properties of sintered permanent magnets.[17–20] Magnetic properties are greatly influenced by temperature and mechanical properties. Sintered NdFeB magnets are typically very hard materials, with a hardness value ranging from 600–700 HV.
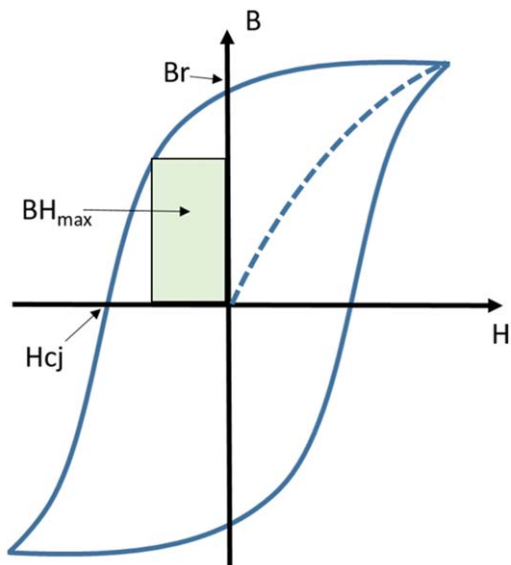
Figure 3. Schematic representation of a permanent magnet hysteresis curve. The green shaded rectangle represents the maximum energy product for this magnet.[17] *Reprinted with permission from Elsevier Ltd.*

Besides their high hardness, NdFeB magnets are also relatively brittle materials. They exhibit high tensile and compressive strength. However, their brittleness makes them susceptible to fracture under certain conditions, so proper design considerations are necessary to avoid overloading.[21]

Typical sintered permanent NdFeB magnets are produced by powder metallurgy and chemically composed of about 25–35 wt% of REEs. Their material cost account for up to 70% of the whole magnet or even higher, depending on specific rare Earth elements and their content. Sintered magnets also contain 60–70 wt% of Fe and about ~1 wt% B. Additions of Al and Co up to 3 wt% are common.

The conventional sintered NdFeB magnet microstructure is formed according to the pseudo-binary phase diagram of the NdFeB ternary system (Fig. 4a). The phase responsible for the exceptionally hard magnetic properties is $Nd_2Fe_{14}B$, with lattice constants a = 0.880 nm and c = 1.221 nm, with the easy direction of magnetisation along the *c*-axis. According to the phase diagram, the stoichiometric $Nd_2Fe_{14}B$ compound forms via a slow peritectic reaction between γ-Fe and a liquid phase (L) at 1158 °C (1428 K). A solidified eutectic ($Nd_2Fe_{14}B$, $Nd_{1+\varepsilon}Fe_4B_4$ and Nd_4Fe) can be found at the triple points along the boundaries between the 2:14:1 matrix phase grain. Nd-rich (Nd_4Fe) phase becomes a liquid phase at temperatures above 665 °C (938 K), well below the sintering temperature and wets the surface of the hard magnetic $Nd_2Fe_{14}B$ matrix grains, enhancing densification during the liquid-phase sintering process. The microstructure also includes grains of the $Nd_{1+\varepsilon}Fe_4B_4$ (B-rich phase), which form grain boundaries with both the Nd-rich and matrix phases, as shown by the scanning electron microscopy (SEM) image in Fig. 4b. This phase is ferromagnetic, and its formation ensures that no soft magnetic Fe phases are produced.

In the NdFeB sintered magnets, the composition slightly richer in Nd compared to the stoichiometric $Nd_2Fe_{14}B$ composition is generally used. The Nd-rich phase is non-magnetic and is easy to oxidise; when oxidised, it does not participate in liquid phase formation and causes precipitation of soft magnetic phase (Fe) at the surface of the main phases, which results in a decrease in coercivity. Therefore, the volume fraction of the Nd-rich phase should be as low as possible, and the composition should be close to stoichiometric.[22]

The crystal structure of the $Nd_2Fe_{14}B$ is complex and can be described as alternating layers of iron atoms and a neodymium-boron compound.[23] The unit cell comprises four $Nd_2Fe_{14}B$ molecules, totalling sixty-eight atoms and forming a tetragonal structure. Yttrium (Y) and lanthanides (rare earths) can occupy the sites of Nd, and transition metals such as cobalt can occupy the sites of Fe. Lanthanide elements are added to contribute to the magnetocrystalline anisotropy due to their chemical structure, with the presence of unpaired electrons of the f-orbitals. Non-metal element boron is added to improve cohesion by strong covalent bonding and increase strength and durability.[11]

Corrosion Resistance of Sintered NdFeB Permanent Magnets: Fundamental Studies

Sintered NdFeB permanent magnets are known for their outstanding magnetic properties; however, they possess poor corrosion resistance due to the multiphase microstructural nature of the material (Fig. 4b). All of the magnet materials are corrosion-sensitive. The Nd-rich matrix and the B-rich phases are susceptible to galvanic corrosion, significantly weakening the magnetic
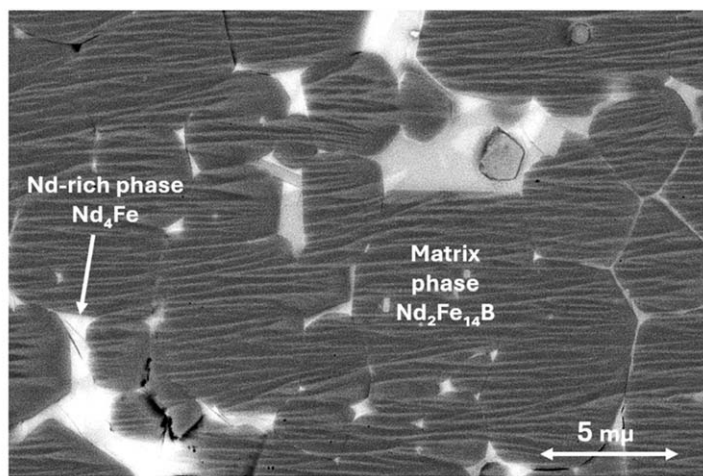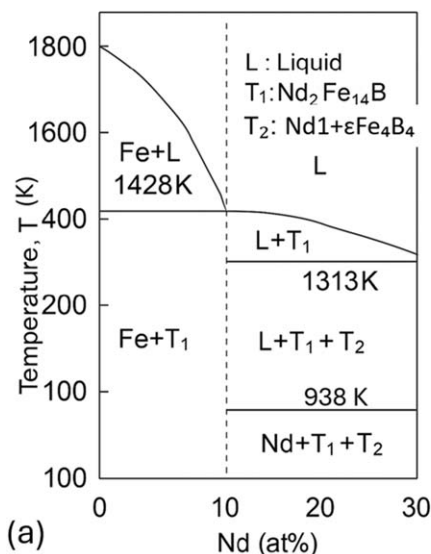

Figure 4. (a) Pseudo-binary phase diagram of the Nd-Fe-B ternary system.[3] l denotes the liquid phase, T_1 and T_2 are the $Nd_2Fe_{14}B$ and $Nd1+_{\varepsilon}Fe_4B_4$ phases. *Reprinted with permission from IOP Publishing Ltd.* (b) Typical microstructure of sintered NdFeB magnets imaged by SEM at 15 kV in a back-scattered electron mode.
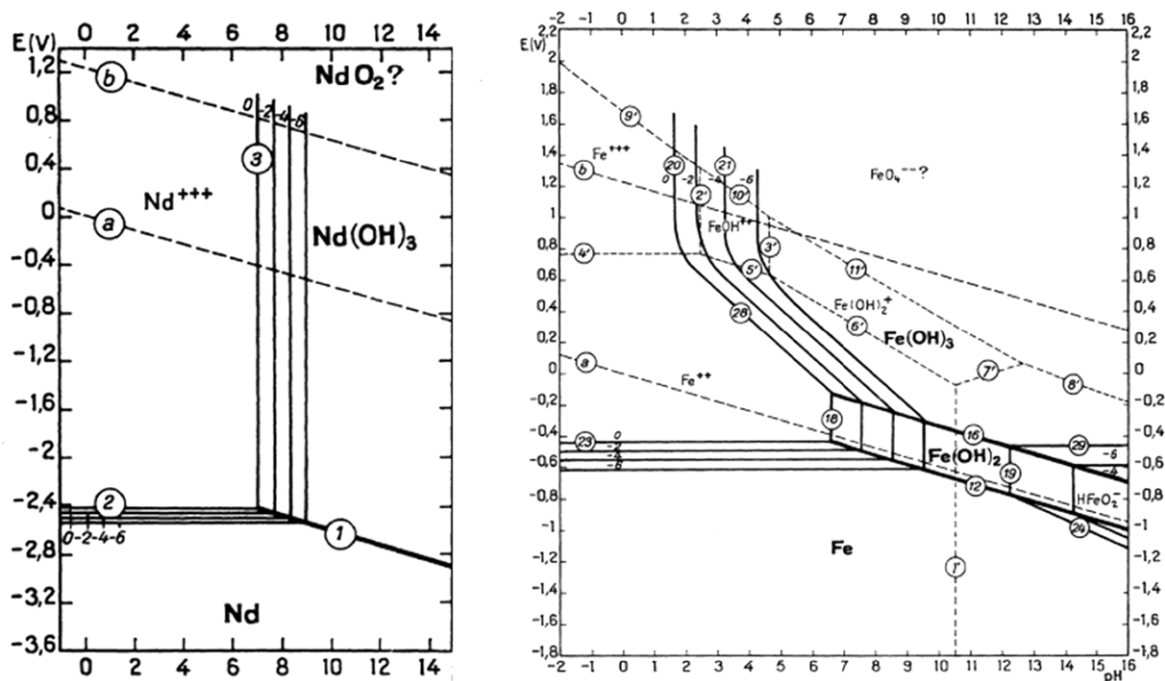
Figure 5. Potential-pH diagrams for neodymium and iron.[25] *Reprinted with permission from the book "Atlas of Electrochemical Equilibria in Aqueous Solutions" by Marcel Pourbaix, NACE, Cebelcor (Houston, Brussels), 1974, publisher National Association of Corrosion Engineers.*

properties and causing failure of the magnets.[24] From the electrochemical point of view, NdFeB magnets have been studied at a relatively basic level. However, understanding these materials' electrochemical and corrosion properties is crucial for developing their corrosion protection and thus prolonging their smooth operation in numerous industrial applications. In this chapter, the fundamental electrochemical results of NdFeB magnets, which were mainly conducted between 2000 and 2010, are summarised depending on the electrolyte. The overview is divided according to the solution pH in which the corrosion studies were made and presented in four main groups: acidic solutions, distilled water, pressurised water or vapour environments, chloride-containing solutions and alkaline solutions.

Figure 5 presents the potential-pH diagrams of Nd and Fe. Neodymium, belonging to the lanthanides, expresses extremely negative equilibrium potentials; its stability domain lies below that of water. Lanthanides are extremely base metals and have a high affinity for reacting with water, which they decompose with the evolution of hydrogen. In the acidic and neutral solutions, Nd dissolves as trivalent cations Nd^{3+}, and in alkaline solutions, it forms Nd(III) hydroxide, $Nd(OH)_3$. Iron dissolves vigorously in acidic, non-oxidising solutions. As the pH increases, the dissolution becomes less vigorous and ceases at pHs above 10 due to the formation of an oxide film. Above pH 13 in non-oxidising solutions, corrosion occurs again.

Corrosion behaviour of sintered NdFeB permanent magnets in acidic solutions.—To determine which phase of the three phases in magnets is mostly susceptible to dissolution, single phases (Nd-rich phase Nd_4Fe, B-rich phase $Nd_{1+\varepsilon}Fe_4B_4$ and matrix $Nd_2Fe_{14}B$) were prepared by melting.[26,27] The corrosion rates of the specimens were determined by a gravimetric method during immersion in N_2-saturated 0.5 M H_2SO_4 at 25 °C (Fig. 6). For the ferromagnetic phase, the corrosion rate increases at a very slow rate. In comparison with these rates, iron corrodes at a rate of only about 0.1 mg cm^{-2} h.[26] For the B-rich phase, two stages of the dissolution process were distinguished. After an initial stage of 4 min in which the corrosion rate increases continuously, a steady state stage is reached. For the Nd-rich phase, the corrosion rate begins at a high value
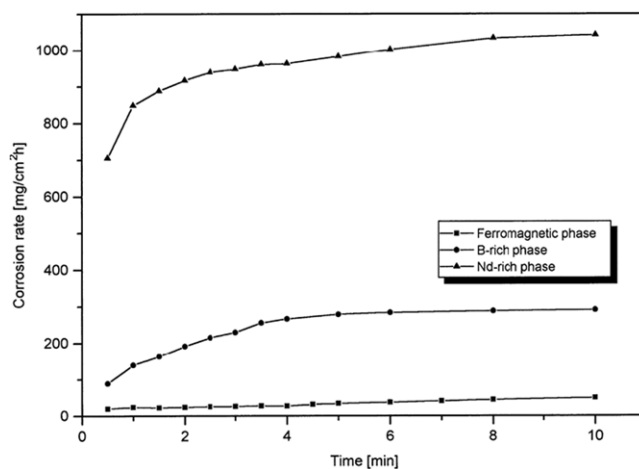
Figure 6. Corrosion rate of single $Nd_2Fe_{14}B$ (magnetic phase), $Nd_{1+\varepsilon}Fe_4B_4$ (B-rich phase) and Nd_4Fe (Nd-rich phase) in N_2-saturated 0.5 M H_2SO_4 at 25 °C as a function of immersion time.[26] The corrosion rate was determined gravimetrically. *Reprinted with permission from Elsevier Science S.A.*

(700 mg cm^{-2} h) and increases quickly. The corrosion rate is lowest for the ferromagnetic phase and highest for the Nd-rich phase. The corrosion rate of the Nd-rich phase is extraordinarily high in comparison with the B-rich phase. Due to this, the Nd-rich phase acts as the anode and the ferromagnetic matrix $Nd_2Fe_{14}B$ phase as the cathode. The susceptibility to dissolution increased in the following order for the non-coupled single phases: ferromagnetic phase < B-rich phase < Nd-rich phase. When two phases were coupled, the differing electrochemical potentials of the three phases primarily result in galvanic corrosion, where intergranular regions of more negative electrochemical potentials of the Nd and B-rich areas are attacked first, causing their anodic dissolution (Fig. 6).

$Nd_2Fe_{14}B$ is surrounded by intergranular regions consisting of the Nd-rich phase Nd_4Fe and the B-rich phase $Nd_{1+\varepsilon}Fe_4B_4$ (Fig. 4b). The corrosion process of sintered NdFeB magnets in H_2SO_4 acidic solutions is characterised by three stages (Fig. 7). The first stage,
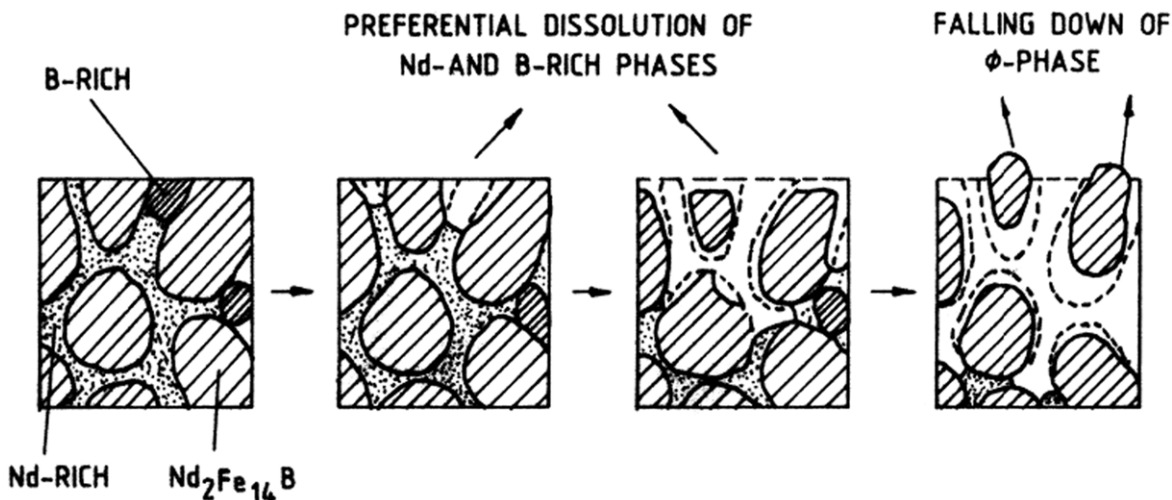
Figure 7. Graphical representation of the degradation of sintered NdFeB magnets in acidic environments.[26,30] *Reprinted with permission from Elsevier Science S.A.*

lasting 1–3 min is the preferential attack on the Nd-rich intergranular region, which primarily occurs due to galvanic interactions with the matrix phase. In the second stage, a rapid increase in the corrosion rate takes place, driven by the preferential dissolution of the Nd-rich intergranular regions and partial undermining of the matrix phase particles. After 6–7 min the corrosion rate reaches a steady state, resulting from the complete undermining and detachment of matrix particles that lose contact with the bulk magnet surface.[28,29]

The area ratio between Nd/B-rich and matrix phases favoured the latter, establishing a corrosion cell of a big cathode/small anode.[30] This kind of system would further accelerate the dissolution at the anode. The cathodic currents are related to the evolution of hydrogen. The hydrogen may be absorbed partly by the phases and cause hydrogen embrittlement. Over time, this leads to the detachment of matrix phase grains from the material surface, resulting in visible material degradation, also called cathodic pulverisation. The neodymium phase is most susceptible to this hydrogen effect. Once hydrogenation occurs, the magnet's surface layer exhibits reduced intrinsic coercivity, making this region more vulnerable to demagnetisation.

Figure 8 compares potentiodynamic polarisation curves of magnets in different acidic solutions, including strong (hydrochloric, nitric and sulphuric) and weak (phosphoric and oxalic) acids.[31]

Hydrogen evolution was identified as the dominant cathodic reaction.[32,33] An active dissolution in HCl, HNO_3, and H_2SO_4 solutions governed the onset of the anodic branch. The current density rose rapidly with increasing anodic potential, leading to the establishment of the diffusion-controlled plateau at more anodic potentials. The corrosion current in the strong acidic solutions of similar hydrogen ion concentration is in the order of HCl > H_2SO_4 > HNO_3.[31,34] On the other hand, in H_3PO_4 and $H_2C_2O_4$, the sintered NdFeB magnets exhibited the typical polarisation behaviour of an active-passive metal, indicating that these two acids passivate the magnet and thus retard corrosion (Fig. 8). However, when the concentration of $H_2C_2O_4$ was too big, extra H^+ would conversely etch the passivation film ($H_2C_2O_4$ is also used as a component of rust-cleaning detergents). Consequently, the passivation effect has a very fragile balance.[31,32] In H_3PO_4, the curve shows an apparent passivating effect, and corrosion is retarded. Phosphate treatment was reported to improve the corrosion resistance of NdFeB-sintered magnets by forming a phosphate layer on the magnet surface.[35]

Corrosion behaviour of sintered NdFeB permanent magnets in liquid, pressurised vapour and water as vapour.—The thermodynamic data govern the electrochemical activity of magnets and depend on the type of environment and its pH value, as predicted by
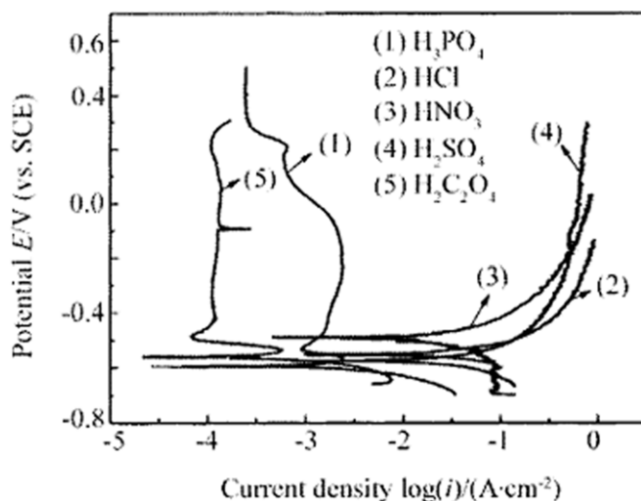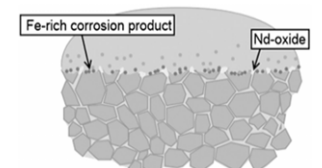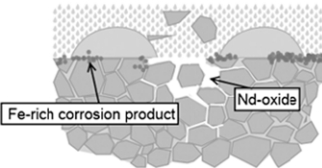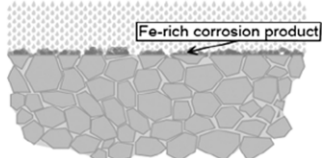
Figure 8. Potentiodynamic polarisation curves of NdFeB sintered magnets in different acidic solutions (phosphoric, hydrochloric, nitric, sulphuric and oxalic acids).[31] *Reprinted with permission from Elsevier B.V. and Science Press.*

the Pourbaix diagrams (Fig. 5). Three media are considered: liquid deionised water, pressurised water vapour and water as vapour (Table I). When a sintered NdFeB magnet is immersed in liquid deionised water, with a pH higher than 5, the Nd-rich phase becomes more corrosion-resistant than the matrix $Nd_2Fe_{14}B$ phase. The Nd-rich phase presented a nobler character by forming more stable Nd-oxides/Nd-hydroxides and acting as a cathode, where an oxygen reduction reaction occurs. Water etches a layer of the matrix grains evenly, leaving the grain boundaries intact, forming a net-shaped structure on the surface of the magnet with red rust, an iron-rich corrosion product.[36,37] After immersion of the sintered NdFeB magnet in deionised water for at least 1 min some tiny pits appeared in the matrix phase near the phase boundary of the Nd-rich phase. With increasing immersion time, these local small pits expanded to the main matrix phase and merged into larger ones. The amount of dissolved oxygen in the liquid is greater than in the humid environment and is sufficient to cause anodic dissolution of the $Nd_2Fe_{14}B$ matrix phase.

In contrast, pure water vapour promotes corrosion of the Nd-rich grain boundary phase.[38] In the presence of the pressurised water vapour, usually done with PCT (pressure cooker test) using pressure

Table I. Corrosion mechanisms in three different types of aqueous environments. *Schemes adapted with permission from* Elsevier B.V.

Type of the aqueous environment	Description of the NdFeB magnets' surface corrosion status	Schematic model for the corrosion mechanism (after 96 h in different accelerated conditions)[36]
Immersion in liquid water	The Nd-rich phase is covered with oxide and becomes a cathode, and the matrix phase becomes an anode. An evenly etched matrix grain layer is formed as a net-shaped structure on the surface.	
Pressurised water vapour	The Nd-rich phase becomes an anode, and corrosion propagates along grain boundaries. The cathodic matrix phase can absorb the reduced nascent hydrogen atoms. Pitting corrosion develops.	
Water vapour/humid environment	The Nd-rich phase becomes the anode, and the Fe-rich phase is the cathode. An even corrosion layer is formed.	
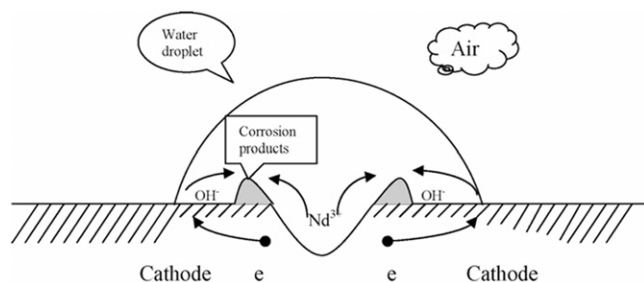
Figure 9. Vertical section sketch of the mechanism for pitting of the NdFeB magnet because of differential aeration beneath a water droplet.[39] *Reprinted with permission from* Elsevier B.V.

vessels partially filled with water and at 120 °C, condensation of water droplets occurs on the Nd-rich grain boundaries at the surface of the magnet (Fig. 9). Water vapour represents the most aggressive corrosion environment for the NdFeB magnets. Selective corrosion of the grain boundary phase and general corrosion of the $Nd_2Fe_{14}B$ grains. Detachment of the latter leads to pulverisation. Pitting corrosion takes place under the condensed droplet surface. The consumption of oxygen in the cathodic reaction in a neutral solution leads to a gradient in oxygen concentration across the water droplet or electrolyte. Oxygen diffuses more readily to the edge of the droplet—where it is in contact with air—compared to the centre, resulting in a higher concentration at the perimeter than at the centre. The Nd-rich phase becomes the anode and is oxidised to cations Nd^{3+}, which react with OH^- ions formed at the cathode or in the water, producing an insoluble $Nd(OH)_3$ precipitate (Fig. 9). This corrosion product forms a ring around the droplet's edge. Simultaneously, hydrogen ions from water dissociation are reduced on both the B-rich phase and the $Nd_2Fe_{14}B$ matrix phase. Some resulting hydrogen may be released as H_2, leading to the disruption of the corrosion layer. Additionally, some nascent hydrogen atoms from the cathodic reduction of water are absorbed by the $Nd_2Fe_{14}B$ matrix, causing lattice expansion and fracturing of this hard magnetic phase.[39,40]

Pure water vapour/humid environment results in the mildest form of corrosion, where the magnet experiences mainly general surface corrosion. Iron-rich red corrosion products gradually cover nearly the entire magnet surface, though material loss after removing these

products remains minimal. Grain-boundary corrosion was observed only in certain localised areas on a microscopic scale. The Nd-rich phase oxidises, while the iron and boron-rich matrix phases act as cathodes. This anodic activity of the Nd-rich phase contributes to forming corrosion products, such as $Nd(OH)_3$, around areas where Nd is exposed.[36] In humid air at 5 bar at 150 °C, single phases follow the same trend as in sulphuric acid, with the Nd-rich phase showing the greatest weight loss.[26] Corrosion of NdFeB magnets was studied in oxidising environments containing controlled additions of water vapour at temperatures up to 150 °C.[41] No significant corrosion was observed in dry environments, but much higher corrosion rates were observed with the increasing humidity of gas mixtures.

Table I summarises the corrosion mechanisms of all three types of aqueous environments.

Corrosion behaviour of sintered NdFeB permanent magnets in chloride-containing environments.—Given that the corrosion of NdFeB magnets poses significant challenges in industrial, marine, and automotive settings, tests conducted in aerated, neutral NaCl electrolytes will likely better reflect realistic conditions. The corrosion sensitivity of the uncoupled single phases in NaCl can be ranked as follows: ferromagnetic matrix phase < B-rich phase < Nd-rich phase. In the absence of occluded cells, such as pits, and with the bulk environment being near-neutral pH, intergranular corrosion is unlikely to be significant.[42,43] But the surface of sintered NdFeB magnets usually contains imperfections such as cracks, inclusions and pores, where chloride ions can adsorb, leading to the decrease in pH and formation of soluble corrosion products in the form of $FeCl_3$ and $NdCl_3$. The autocatalytic reaction of corrosion and dissolution, thus initiated, results in pitting corrosion.[32,44] Meanwhile, some matrix phase grains crack along the grain boundaries and intergranular corrosion appears. The ferromagnetic matrix phase detaches from the magnet's surface, thus exposing the fresh underlying layer. This corrosion behaviour was previously defined in literature as layer-by-layer corrosion.[45] The oxide/hydroxide layers are formed in a net-like structure, stable to certain chloride concentrations.[46–48] Figure 10 shows potentiodynamic curves of NdFeB magnets in NaCl solutions of different concentrations. The anodic side displayed a similar shape to that in the HNO_3 solution, both primarily showing an active corrosion region followed by a diffusion-controlled current density plateau. However, the
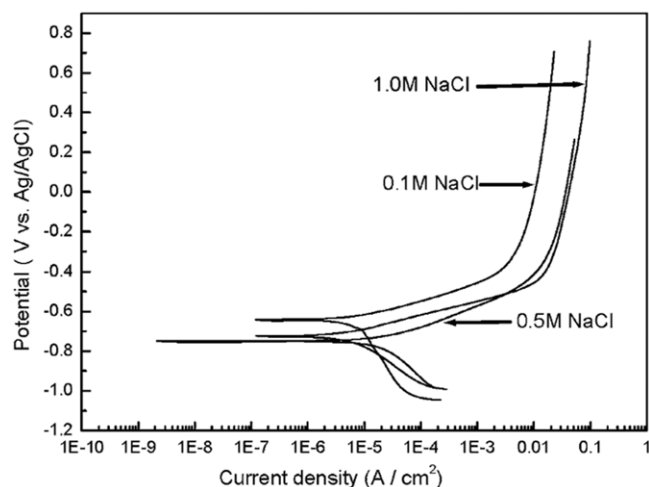
Figure 10. Potentiodynamic curves of NdFeB magnets in NaCl solution.[32] *Reprinted with permission from Wiley-VCH.*

Figure 11. Potentiodynamic curves of sintered NdFeB permanent magnets in alkaline NaOH solutions.[32] *Reprinted with permission from Wiley-VCH.*

corrosion current density (j_{corr}) was noticeably lower than, for example, in HNO_3 (Fig. 8), suggesting that NdFeB experiences only a limited degree of attack in NaCl solution of near-neutral pH. The increase in chloride concentration to 0.5 M intensified the corrosive attack. However, 1.0 M NaCl surprisingly exhibited weaker corrosive effects on NdFeB than 0.5 M NaCl. This phenomenon is linked to the mechanism of oxygen adsorption during corrosion. In neutral or alkaline solutions, the primary cathodic reaction is according to reaction 1:

$$O_2 + 2H_2O + 4e^- \rightarrow 4OH^- \qquad [1]$$

The corrosion rate is governed by the diffusion of oxygen from the solution to the substrate surface. A higher NaCl concentration reduces the amount of dissolved oxygen, thereby inhibiting the anodic dissolution reaction. Consequently, 0.5 M NaCl displayed the most aggressive corrosion behaviour on NdFeB magnets.[32]

Corrosion behaviour of sintered NdFeB permanent magnets in alkaline solutions.—In the alkaline NaOH media, the NdFeB sintered magnet's surface passivates spontaneously, as expected based on the Pourbaix diagrams (Fig. 5). No apparent effect on the polarisation curves was noticed because of the change in NaOH concentration (Fig. 11). The anodic side shows the transition from the active region to the passivation region and then to the trans-passivation region at potentials more positive than 0.6 V vs Ag/AgCl. In the alkaline solution, the hydroxyl ions contribute to the formation of a compact passivation film according to reactions 2 and 3:

$$Fe^{3+} + 3OH^- \rightarrow Fe(OH)_3 \qquad [2]$$

$$Nd^{3+} + 3OH^- \rightarrow Nd(OH)_3 \qquad [3]$$

The growth rate of the hydroxide passivation film seems considerably slow.[32] It was shown that only comparatively high concentrations of chloride or sulphate ions can induce the breakdown of passivity, i.e. for $\geqslant 0.1$ M of Cl^- and $\geqslant 0.5$ M SO_4^{2-} at potentials above 1 V (SHE). The breakdown of passivity begins with the initiation and spread of cracks in the passive layer, likely affecting the neodymium as well.[49] Once pitting is initiated, a lowering of the potential by reverse dynamic scanning does not lead to re-passivation.

Corrosion behaviour of sintered NdFeB permanent magnets in automatic transmission fluids.—Automatic transmission fluids (ATF) are complex mixtures (Table II) containing various additives
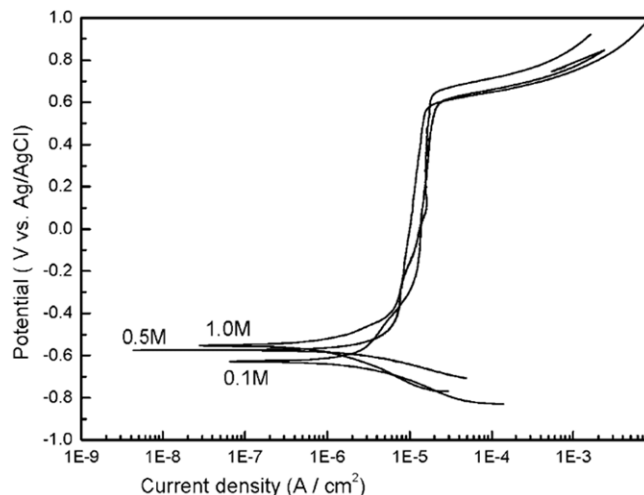
designed for the performance of the electromotor. The compounds react with each other to form a stable lubricant surface.

Hydrocarbons in mineral oil themselves do not cause corrosion, but the presence of water content, sulphur molecules and acid compounds can cause a chemical attack on the surface of sintered NdFeB magnets and their coatings.[51] Therefore, additives can be chemically aggressive, potentially exacerbating the corrosion of NdFeB magnets.

Most of the literature sources are focused on sulphur compounds (such as H_2S, SO_x), which are inherently contained in the purified mineral oil and originate from the ATF compositions; however, sulphur compounds are highly corrosive to the metal of electric circuits and also NdFeB magnets.[52] After exposing materials to higher temperatures, extended periods, and water/humidity, volatile sulphide compounds were analysed in ATF.[53] These included hydrogen sulphide (H_2S), carbonyl sulphide (COS), carbon disulphide (CS_2), and sulphur dioxide (SO_2). At temperatures higher than 140 °C, the amount of sulphide compounds doubled within a short time.[50] Water and O_2 are reacting with SO_2 to form H_2SO_4 and consequently form an acidic, corrosive environment. The Nd-rich phase is galvanically attacked, and intergranular corrosion takes place preferentially. Metals in contact with ATF, such as copper, aluminium, and steel, are subjected to mixed types of corrosion, and pitting areas are preferentially noticeable.[53,54]

A substantial loss in coercivity was observed for melt-spun NdFeB magnetic powder when aged for 1000 h in ATF at 150 °C, which was ascribed to hydrogen dissociated from ATF and entering the $Nd_2Fe_{14}B$ lattice.[55]

The contemporary manufacturing and recycling processes of sintered NdFeB permanent magnets.—The ideal NdFeB magnet would consist of small, regular-shaped grains of $Nd_2Fe_{14}B$, all with their easy axis of magnetisation aligned. The matrix phase grain size should be as small as possible to reduce the formation of nucleate domains under the influence of the outer reverse field. Additionally, by isolating each grain with a thin layer of non-magnetic (mainly Nd-rich) grain boundary phase, reverse domains[a] cannot spread easily through the bulk sample.[56,57] These conditions must be fulfilled to give a magnet good remanence (grain alignment factor) and high coercivity (smooth, well-isolated grains). In the last 20

---

[a] In a magnet, "aligned domains" and "reverse domains" refer to the microscopic arrangement of magnetic moments within the material. "Aligned domains" are regions where the atomic magnetic moments are all pointing in the same direction, creating a net magnetic field. "Reverse domains" are regions where the atomic magnetic moments are pointing in the opposite direction, effectively counteracting the aligned domains; reverse domains can cause demagnetisation. The magnet is anisotropic if all domains are aligned in the same direction. It contributes to their high coercivity and resistance to demagnetisation.

Table II. Formulation of typical ATFs.[50] *Reprinted with permission from the* IEEE.

Component	Content (wt%)	Compound
Base oil		Mineral oil
Antiwear	1	Phosphate, ZnDTP[a]
Dispersant	2–10	Calcium sulfonate
Friction modifier	0.4–2	ZnDTP[a], organo-molybdenum compounds, etc.
Antioxidant	0.4–2	Alkyl phenol
Rust inhibitor	0.1–1	Phosfate
Antifoamer	0–0.1	Silicone
Viscosity modifier	2–10	Polymethacrylate

a) ZnDTP is zinc dialkyl dithiophosphate.

years, tremendous progress has been made in the magnet production process, including different strategies/methods to enable better magnetic properties of the NdFeB magnets. Modern ways of magnet production are shown (Fig. 12). Technological progress has enabled the reach of high magnet energy products, which are the consequence of the above-mentioned near-ideal magnet microstructural properties. In this section, contemporary production methods aimed at microstructural modifications are summarised, followed by a section describing how these modifications, along with surface treatments, affect the corrosion resistance of the magnets.[1,14,58,59]

The manufacturing process starts with the melting of the starting material that comprises good intrinsic properties; the goal is to translate these into functional extrinsic properties of a new magnet. According to the phase diagram (Fig. 4a), Fe precipitates as a primary phase from molten alloy during the casting process of NdFeB magnets and tends to become a nucleation site of reverse domains. This is why the precipitation of a primary Fe should be inhibited during the ingot fabrication process. To achieve that, strip casting (SC) is used as an advantageous process step that enables a very homogenous microstructure with NdFeB grains ($Nd_2Fe_{14}B$ and Nd-rich phase) in the grain microscale of 4–6 μm. SC-produced material has a columnar structure of $Nd_2Fe_{14}B$ and Nd-rich phases; it is additionally crushed and milled to form a fine powder size, suitable for the sintering process step (1030 °C–1080 °C). All production steps are done under a controlled atmosphere.[59–63]

Instead of mechanical ingot crushing, a hydrogen process called hydrogen decrepitation (HD) is used later.[64] HD is an alternative method for producing powder to manufacture sintered NdFeB magnets.[65] In this process, NdFeB-type material is exposed to gaseous hydrogen at atmospheric or elevated pressure and room or elevated temperature. The hydrogenation induces stress due to the volume expansion of the hydrogenated phases, causing the material to fracture and break down into smaller particles. Consequently, the HD process enables the transformation of bulk NdFeB ingots into a friable powder.

A jet mill (JM) is widely used to fabricate even finer powders. Inside, a compressed inert gas vortex is created, which results in particle-on-particle impact. Material is ground to 3–5 μm with a very narrow powder size range without contamination or oxidation. Additionally, powder aligning in the magnetic field to achieve magnetisation, pressing, sintering, and annealing processes have been significantly improved. Sintering occurs at elevated temperatures for several hours (1000 °C–1100 °C) and is followed by post-sinter annealing (∼600 °C) to refine the grain boundary texture and relieve internal stresses. During sintering and annealing, the atmosphere is severely controlled, and recent high-performance nanocrystalline NdFeB magnets were produced without any air exposure during manufacturing.
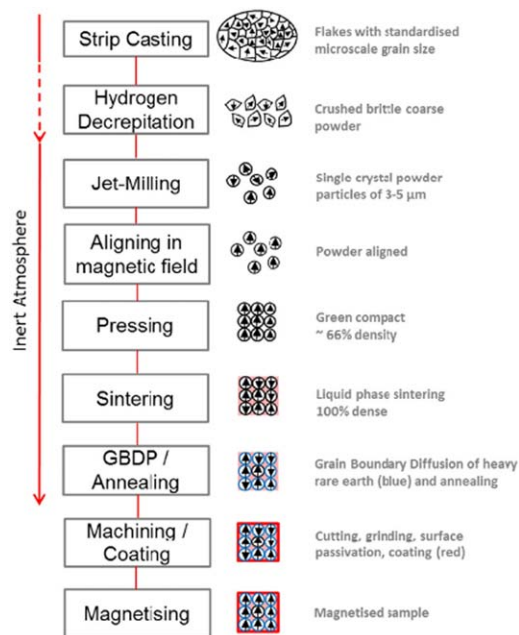

Figure 12. Schematic of the modern manufacturing process steps of the sintered NdFeB magnet.[5] *Reprinted with permission from Springer Nature.*

In terms of production method, hot-deformed magnets should be mentioned in addition to sintered and bonded magnets. In contrast to sintered magnets, where the crystallographic alignment is achieved via magnetic alignment (Fig. 12), in hot-deformed magnets, it is achieved via plastic deformation at high temperatures.[66,67] Powders of $Nd_2Fe_{14}B$ are first cold-pressed and then hot-pressed at 650 °C–700 °C to obtain an isotropic dense magnet with a small grain size in the range of 50 nm. This step is followed by hot plastic deformation at 750 °C–850 °C, where the material becomes anisotropic with highly oriented platelet-like grains sized 200–400 nm and 50–80 nm thick.

NdFeB sintered magnets are the strongest type of permanent magnets, but they start to lose magnetic properties with increasing temperature, i.e. from 80 °C to 150 (200) °C; the reason lies in their low Curie temperature (the temperature at which a material loses its magnetism) of about 310 °C.[68] This is one of the drawbacks of NdFeB magnets. In contrast, SmCo-based magnets, although with a lower coercivity, have higher temperature stability, with operating temperatures up to 550 °C and a Curie temperature between 700 and 800 °C. Therefore, the temperature dependence of NdFeB magnets' coercivity is significant, but for advanced magnet use, high thermal stability is crucial. Sintered magnets exhibit distinct brittleness, making the material susceptible to fracturing.

There are several methods to increase mechanical properties and temperature stability (Fig. 13) by decreasing the possibility of multi-domain structures forming in sintered magnet material (with a high coercivity). They are primarily focused on the grain boundaries (GBs) engineering.[69] Namely, in NdFeB magnets, the coercivity is controlled by the properties of the intergranular regions around several micrometre-sized $Nd_2Fe_{14}B$ grains. In particular, Nd-rich grain boundaries play a critical role. Therefore, by controlling the interfacial microstructure between the matrix $Nd_2Fe_{14}B$ phase and an Nd-rich phase, the interface is strengthened. Defects at the surface of the matrix phase are the starting weak point for magnetic reversal domains, known as the nucleation model of the coercivity mechanism of NdFeB magnets.[3,5] The GB engineering comprises grain boundary diffusion processes (GBDP) aiming to optimise grain boundary microstructure and intergranular addition (so-called dual-alloy method), as schematically presented in Fig. 13.
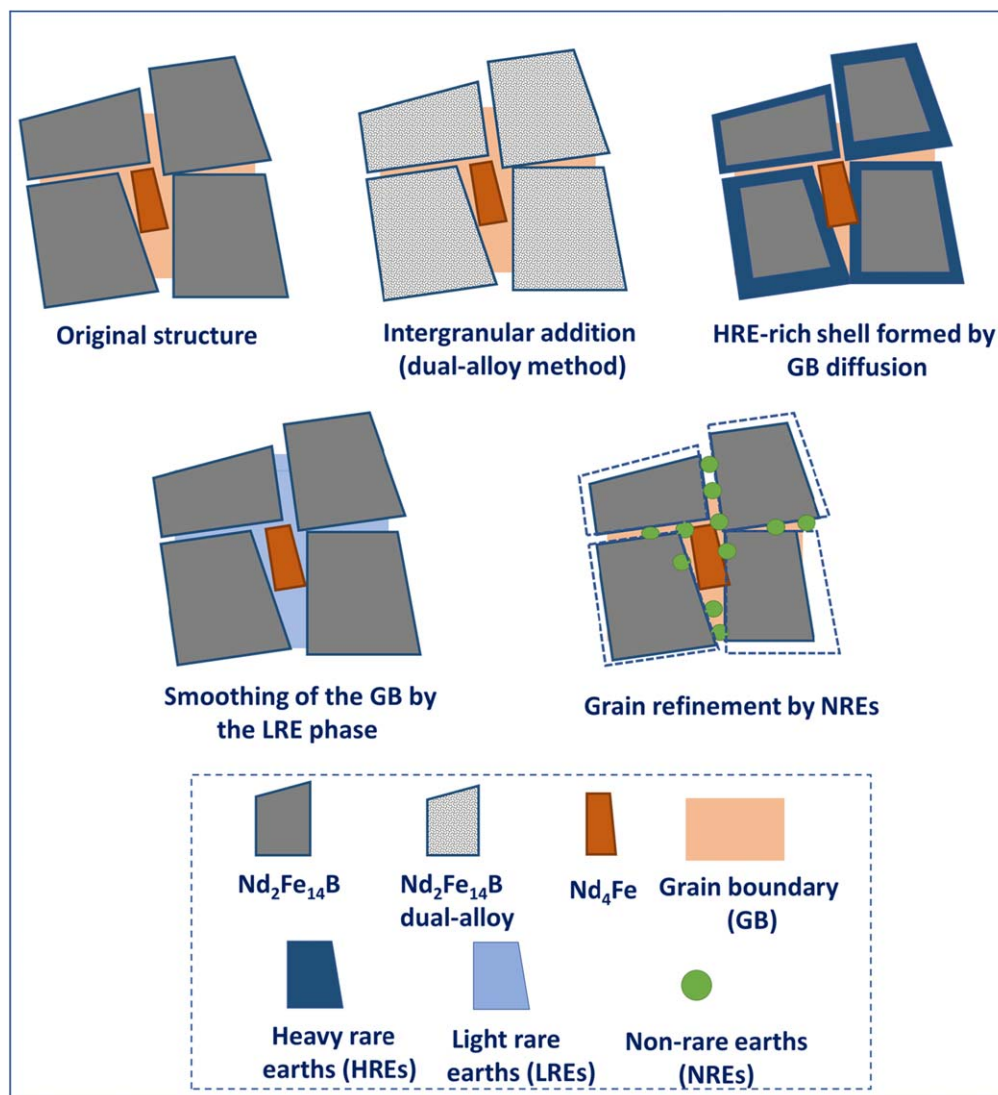
Figure 13. Schematic presentation of the main approaches of intergranular addition and grain boundary diffusion modifications.

The GBDP was based on the observation that the coercivity of the magnet, coated with heavy rare earth (HRE = dysprosium (Dy) and terbium (Tb)) oxide or fluoride powders and then heat-treated, was enhanced significantly.[12,70] The heat treatment temperature for the HRE diffusion in the GBDP is relatively low, and new technologies that allow controlled HRE quantity and distribution during diffusion were later developed. This compositional modification by HRE metals and compounds (Dy, Tb, Dy_2O_3, DyF_3, TbH_3) represents the first-generation GBDP, where HRE diffusion infiltrates from the surface through the grain boundary into the interior of the magnet, forming an HRE-rich shell through the melting/solidification of an HRE-rich intermediate phase during heat treatment. The content of HRE decreases from the surface into the bulk (Fig. 13). Lanthanides Nd^{3+}, Dy^{3+}, Tb^{3+} and Pr^{3+} have similar electronic configurations so that the strong uniaxial anisotropy in the Nd_2F_{14}-phase is retained when Nd^{3+} is replaced by some of these cations.[11]

The material for GB diffusion is prepared in different ways, e.g., as a powder suspended in alcohol into which the magnet is immersed, followed by diffusion heat treatment or as a coating deposited onto the magnet, followed by heat treatment to achieve inward diffusion (see below Table IV). Different ways to vapourise or ionise the material source for diffusion include electrodeposition, sputtering and ion plating.[71–75] Another way of GB modification is

the intergranular addition, where HRE metals or compounds are firstly blended with NdFeB powder (alloying), and then in situ diffusion occurs during sintering (so-called dual-alloy method).[74]

The price of HREs and their low abundance led to the second generation GBDP focused on light REs (LREs), which are found at a higher abundance and are cheaper. The aim is to use Dy/Tb-free magnets at very low or even no HRE metals. The LREs are used as grain boundary diffusion sources in the form of low-melting eutectic alloys based on praseodymium (Pr) and neodymium (Nd), i.e., Pr−M and Nd−M (M = Al, Cu) and lanthanum (La) and cerium (Ce), i.e., La−M, La−Ce−M (M = Al, Cu). Elements like Cu and Al form eutectic phases with Nd and Fe and lower the melting point of the GB phase.[74] The role of LREs is to smooth the GB defects and thicken the GB phase, thus isolating the magnetic grains.

The optimisation of the GB phase distribution is the focus of the third-generation GBDP based on non-RE elements, i.e. oxides of Cu, Al, Ni, Mg and Zn (Fig. 13). The mechanism is based on the substitution of Nd−O−Fe intergranular phase by Nd−O−Fe−M (M = Al, Mg, Zn, Cr and Ca). These particles distribute along the GB, increasing the coercivity and hindering the intragranular propagation of reversal domain walls, which negatively impacts the magnet behaviour. Two types of non-RE additives are distinguished. (i) Elements Al, Cu, Zn, Ni, and Mg, which improve the wettability of the GB phase with the $Nd_2Fe_{14}B$ phase. As mentioned above, these

Table III. Common additives to magnet materials and their effects.[5,59]

Additive element	Role of additives and their influence on magnetic properties
Dysprosium (Dy) and Terbium (Tb)	Substitutes for Nd are placed at the edges of the matrix grain to increase the anisotropy and coercivity of the magnet and to withstand higher operating temperatures.
Niobium (Nb) and Vanadium (V)	Grain refinement and improvement of H_{cj} due to reduced grain growth in sintering.
Copper (Cu) and Aluminium (Al)	Improves wetting during sintering and effects in lower B_r due to the formation of non-magnetic phases, improves H_{cj} due to isolation smoothing.
Cobalt (Co)	Nd_3Co phases form at the grain boundary, and Co is substituted for Fe in the matrix, resulting in increased Curie temperature of the $Nd_2Fe_{14}B$ phase, increased B_r and decreased H_{cj}.
Niobium (Nb) and Vanadium (V)	Borides form at grain boundaries, which causes grain refinement. H_{cj} is improved due to reduced grain growth in sintering.
Gallium (Ga)	Increases H_{cj} and hot workability of the alloy.
Gadolinium (Gd)	Increases the temperature coefficient.

elements form the eutectic phase, which enters the gap between the $Nd_2Fe_{14}B$ grains and forms a thin layer during sintering, thus isolating the hard magnetic. (ii) Elements like molybdenum (Mo), tungsten (W), niobium (Nb) and tantalum (Ta) inhibit the grain size growth, resulting in grain refinement.[76] Generally, smaller grain sizes lead to higher coercivity and better thermal stability, while larger grain sizes can affect remanence and corrosion resistance. For example, adding a small amount of Nb inhibits the grain growth of the matrix phase and also improves strength and toughness (Table III). Until now, non-RE diffusion sources still have a less positive effect on the coercivity enhancement of magnets compared to RE-based sources.[71,73,74,77–79]

In commercial sintered NdFeB magnets, the Nd element is usually partially substituted by other rare earth elements, including Pr, Dy, Tb, etc. Because Nd and Pr elements usually coexist in ore and have similar physical and chemical properties, it is more economical to produce PrNd alloy instead of pure Nd metal from ore and to use PrNd alloy as the raw material for magnet production. Dy and/or Tb element substitution for the Nd element can remarkably increase the intrinsic coercivity due to their higher magnetocrystalline anisotropy field. These two elements also increase magnets' temperature stability, required for developing markets, such as automotive applications, which must operate up to ~180 °C. Depending upon applications, different elements, such as Dy, Tb, Co, Gd, Cu, Al, Ga and Nb, are added to improve the physical and magnetic properties of the magnet. The roles of some additives on the magnet properties are summarised in Table III.[1,3,58,60,80,81]

Around 23% of the world's rare earth production is consumed for manufacturing only NdFeB magnets. Depending on the applications, NdFeB magnets have 2 to 3 years life cycles in consumer electronics, from 20 to 30 years in wind turbines. Much work has been done recently on recovering rare earth elements from NdFeB permanent magnet scrap.[80] As rare earths of these products do not degrade in their lifetime, end-of-life products could also be an alternative source of these elements. Due to the lack of REEs, and limited sources, a cost-effective recycling process would be a real step forward. The recycling of RE permanent magnets can be based on material recycling by smelting, element recycling by leaching or direct magnet recycling by hydrogen decrepitation. The recycling processes in the recent period show an improvement over the primary production of NdFeB magnets from an economic and environmental point of view. It is estimated that less than 1% of the global recycling rate for used permanent magnets is achieved.[5,62,80,82–85] The magnets are very different in application and size, so having a unified recycling process for all magnet types is hard.[83] Nowadays, numerous research and industrial projects are focusing on this area, aiming to increase the efficiency of recycling processes.

Methods of improving the corrosion resistance of sintered NdFeB magnets.—Testing the corrosion resistance of magnets is usually conducted using non-electrochemical methods, such as salt spray chamber and vapour pressure test (also known as pressure cooker test (PCT) or autoclave test) and electrochemical methods. Some of the most common standards are given in Table IV. Electrochemical methods most commonly comprise the recording of potentiodynamic polarisation (PDP) curves and electrochemical impedance spectroscopy (EIS).

Many efforts have been dedicated to improving the magnetic properties and corrosion resistance of sintered NdFeB magnets, as described in the previous section. Comprehensive reviews[11,23,67,69,76,86] were mainly focused on the former, whereas the reviews dealing primarily with corrosion resistance are lacking.[87] There are two main approaches to improving the corrosion resistance of sintered magnets: (i) modification of the magnet composition and microstructure, and (ii) modification of the magnet's surface by deposition of coatings. The literature review is presented in the following two subsections.

Improvement of corrosion resistance of sintered NdFeB magnets by the modification of the magnet composition and microstructure.—Tables V and VI summarise the studies in which the effect of the modifications of microstructure was studied in relation to the corrosion properties. Table V specifically address the impact of intergranular addition of various elements and sintering methods, whereas Table VI present the studies in which the effect of grain boundary diffusion of rare earths and non-rare earths was addressed. The main findings are summarised in the tables. In the case of dual-alloy intergranular methodology (Table V), the beneficial effects of the addition of Ce, Dy, Ca-Ga, Pr, Pr-Co-Ga, (Pr,Nd)-Al, Pr-Dy-Nb, Cu-Al, Ni-Cr and Nd-Co were ascribed to the modification of grain size, reduced activity of the RE-phase, decreasing the potential difference between the Nd-rich phase and the matrix, change in the distribution of intergranular phases, improvement of the uniformity of the Nd-rich phase, and reduction of the number of active reaction channels. Some examples of the improvement of corrosion resistance are presented in Fig. 14.

NdFeB magnets can be made more corrosion-resistant by positively shifting the open circuit potential (OCP) of the Nd-rich phase, thus decreasing the electrochemical potential differences between the magnet's phases. For this purpose, different alloying additions were tested, including Co, chromium (Cr), Cu, Ga, Al, Ce and holmium (Ho).[28,118–126] Some of the mentioned additions can also improve magnetic properties and thermal stability, and reduce the cost of raw materials. However, refining the microstructure leads to higher corrosion rates since there is more Nd-rich phase between grains, which is electrochemically less stable.[127] Also, corrosion susceptibility increases with decreasing density.[40]

In the second approach, i.e., GB diffusion of REs and non-REs, the improvement of corrosion resistance was ascribed to the enrichment of the grain boundary shell by Dy, Tb, Dy-Co, Tb-Ga, Pr-Tb-Ni-Cu, Ni-alloyed Dy-Co, Al, MgO, ZnO and NbC (Table VI). Some examples of the improvement of corrosion resistance are presented in Fig. 15.

Table IV. Most common standardised methods for non-electrochemical and electrochemical testing. ISO - International Organization for Standardization; ASTM International - American Society for Testing and Materials; IEC - International Electrochemical Commission; NACE - National Association of Corrosion Engineers.

Standard	Title
Non-electrochemical methods	
ISO 9227–2006	Corrosion tests in artificial atmospheres
ASTM B 117–07a	Standard practice for operating salt spray (fog) apparatus
IEC 60068-2-66: 1994	Environmental testing—Part 2: Test method—Test Cx: Damp heat, steady state (unsaturated pressurised vapour)
ASTM A1071/A1071M–11 (reapproved 2015)	Standard test method for evaluating hygrothermal corrosion resistance of permanent magnet alloys
NACE TM0168/G31–12a	Standard guide for laboratory immersion corrosion testing of metals
ISO 8407	Corrosion of metals and alloys — Removal of corrosion products from corrosion test specimens
Electrochemical methods	
ASTM G 5–94 (reapproved 2004)	Standard reference test method for making potentiostatic and potentiodynamic anodic polarization measurements
ISO 16773–1 (2016)	Electrochemical impedance spectroscopy (EIS) on coated and uncoated metallic specimens. Part 1: Terms and definitions
ISO 16773–2 (2016)	Electrochemical impedance spectroscopy (EIS) on coated and uncoated metallic specimens. Part 2: Collection of data

Table V. Summary of studies dealing with the corrosion resistance of magnets produced by different sintering methods or modified using intergranular addition.

Short description	Effect on the corrosion resistance and the methodology used	Reference
Intergranular addition (dual-alloy) magnets		
addition of Ce to NdFeB	the addition of Ce leads to grain size reduction and RE-rich phase increases; PDP curves and mass loss in NaOH, HNO_3, HCl, H_2SO_4, $H_2C_2O_4$	Bi 2017[88]
addition of Ce to NdFeB	Ce improves the corrosion resistance by reducing the activity of the RE-phase; PDP curves, EIS spectra and mass loss in 3.5 wt% NaCl	Yang 2017[89]
addition of Ce to NdFeB	mass loss is larger for sintered than for annealed magnet; PCT test and PDP curves in HCl and NaCl	Shi 2023[90]
addition of Dy and Co-Ga to NdFeB powder, hot-pressed and sintered	partial substitution of Fe with Co and Ga improves the corrosion resistance and reduces the affinity for hydrogen; immersion test and PDP curves in H_2SO_4	El-Moneim 2002[28]
addition of Dy to NdFeB, jet-milled, pressurised and sintered	Dy improves the corrosion resistance by reducing the Nd-rich phase and lowering its potential relative to the matrix; PDP curves, EIS spectra and immersion test for 144 h in 3.5 wt% NaCl	Yang 2024[91]
addition of Pr and Pr-Co-Ga to recycled NdFeB powder, crushed using HD, jet-milled and sintered	incorporation of $Pr_{90}Co_8Ga_2$ changes the phase composition by forming a more stable Nd-rich phase containing Ca and Ga; PDP curves in 3.5 wt% NaCl	Huang 2024[92]
(Pr,Nd)-Al blended with (Ce,Pr,Nd)FeB and prepared by powder metallurgy, jet-milled, hot-pressed and sintered	(Pr,Nd)-Al affects the distribution of intergranular phases and improves corrosion resistance; PDP curves and EIS spectra in 3.5 wt% NaCl	Wang 2021[93]
addition of Pr-Dy-Nb and Pr to NdFeB powder, HD, jet-milled and sintered	adding Dy and Nb improves the uniformity of the Nd-rich phase; mass loss during immersion in 3.5 wt% NaCl for 60 days	Zhang 2021[45]
addition of $Cu_{29.8}Al_{70.2}$ ribbons to NdFeB powder, HD, ball-milled, pressurised and sintered	adding $Cu_{29.8}Al_{70.2}$ enhances the Nd-rich phase; PDP curves in 3.5 wt% NaCl and PCT test	Liu 2018[94]
addition of Zr and Ti to NdCeFeB powder, HD, jet-milled, pressurised and sintered	Ti-rich precipitates decrease the amount of active reaction channels; PDP curves and EIS spectra in 3.5 wt% NaCl	Shao 2024[95]
addition of Ni-Cr to recycled NdFeB powder, ball-milled, pressurised and sintered	Ni-Cr modifies the GB; PDP curves, and EIS spectra in 3.5 wt% NaCl	Mehenni 2024[96]
addition of Nd-Co alloy to recycled NdFeB powder, jet-milled, pressurised, and sintered	similar mass loss between fresh and recycled magnets; mass loss (PCT)	Huang 2024[97]
Sintering processing		
effect of pressure holding time on hot-deformed NdFeB	pressure times improved the distribution of active reaction channels; PDP curves in 3.5 wt% NaCl	Li 2024[98]
hot-pressed nanocrystalline NdFeB prepared by melt-spun powders	Nd-rich phase preferentially corrodes in NaCl; simulated marine atmosphere (NaCl of 80% relative humidity)	Zhang 2014[99]
hot-deformed and sintered NdFeB with and without Dy	hot-deformed magnes express better corrosion resistance due to narrower GB width, higher Dy content and lower total RE content; PDP curves in 3.5 wt% NaCl and PCT test	Dai 2023[100]

Table VI. Summary of studies dealing with the corrosion resistance of magnets modified using grain boundary diffusion of rare earths and non-rare earths.

Short description	Effect on the corrosion resistance and methodology used	Reference
Heavy rare earths grain boundary diffusion		
$Dy_{30}Cu_{70}$ powder prepared by arc melting and suspended in ethanol; NdFeB processed in suspension and heat-treated	diffusion of DyCu alloy to GB shell improves the corrosion resistance; PDP curves in 3.5 wt% NaCl	Huang 2022[101]
TbH_3 powder prepared by hydrogen crepitation and ball milling and suspended in ethanol; NdFeB processed in suspension and heat-treated	enrichment of Tb in the GB phase reduces the corrosion rate; PDP curves in 3.5 wt% NaCl and immersion in NaCl at 50 °C	Zhou 2023[102]
TbH_3 powder dip-coated on dual-alloys (Pr,Nd)FeBCoM and (Pr, Nd)DyFeBCoM (M=Cu, Zr, Ga) and heat-treated	enrichment of Tb in the GB phase reduces the corrosion rate; PDP curves in NaCl and immersion in NaCl at 50 °C	Toujun 2023[103]
$Tb_{69}Ni_{31}$ powder prepared by arc melting and suspended in ethanol; (Dy,Pr)NdFeB processed in suspension and heat-treated	Ni-phase formed at grain boundaries improves the corrosion resistance; PDP curves and EIS in 3.5 wt% NaCl	Zhang 2025[104]
Dy-electrodeposited on NdFeB and heat-treated	infiltration of Dy in GB shell decreases corrosion current density; PDP curves in 3.5 wt% NaCl	Yan 2024[105]
Dy electrodeposited on NdFeB and heat-treated	infiltration of Dy in GB shell decreases corrosion current density; PDP curves in 3.5 wt% NaCl	Yan 2024[106]
Tb-Ga electrodeposited on NdFeB and heat-treated	infiltration of Tb and Ga in GB shell decreases corrosion current density; PDP curves and EIS in 3.5 wt% NaCl	Wang 2025[107]
Dy and DyAl magnetron-sputtered on NdFeB and heat-treated	$Dy_{95}Al_5$ − NdFeB exhibits enhanced electrochemical stability and optimises the distribution of intergranular phases; PDP curves in 3.5 wt% NaCl	Tang 2024[108]
TbF_3 electrodeposited on NdFeB and heat-treated	the formation of the surface oxide layer and reduction of interphase potential difference; PDP curves in 3.5 wt% NaCl and SEM analysis	Shi 2025[109]
Ni-alloyed Dy-Co ribbons prepared by arc-melting, covered onto NdFeB and heat-treated	addition of Ni decreased corrosion current density; PDP curves and EIS in 3.5 wt% NaCl	Cao 2024[110]
TbH_x and TbF_3 powders prepared by evaporation and condensation or sand milling, suspended in alcohol, electrophoretically-deposited onto NdFeB, and heat-treated	diffusion of Tb reduced the interphase potential difference between phases; PDP curves and EIS in 3.5 wt% NaCl, salt spray chamber test	Ji 2025[111]
Non-rare earths grain boundary diffusion		
Al film prepared by magnetron-sputtered onto NdFeB and heat-treated	Al diffusion decreases the corrosion current density; PDP curves and EIS in 3.5 wt% NaCl	Chen 2019[112]
addition of In NdFeB, jet-milled and sintered	In-precipitates hinder the ingress of corrosion medium; PDP curves in 3.5 wt% NaCl	Li 2024[113]
addition of MgO and ZnO to NdFeB, ball-milled and sintered	MgO and ZnO incorporate into the intergranular phase, increasing the fraction with higher oxygen content, leading to better corrosion resistance; PDP curves in NaH_2PO_4, $NaCl+MgCl_2$ and PCT test	Mo 2008[114]
addition of Nb to NdFeB, gas-milled and sintered	Nb optimises the distribution of Nd-phase and refines the grains; immersion in 3.5 wt% NaCl for up to 50 days	Zhang 2023[115]
ZnO magnetron-coated onto NdFeB and heat-treated	the formation of oxides at the triple junction of grains enhances the corrosion resistance; PDP curves and EIS spectra in 3.5 wt% NaCl	Wang 2021[116]
NbC powder added to NbFeB ribbons, hot-pressed and sintered	barrier effect of NbC on Fe/Nd oxidation and hindrance on active reaction channel formation; PDP curves and EIS spectra in 3.5 wt% NaCl	Song 2025[117]

Finally, it was observed that corrosion was significantly accelerated when the magnets were tested in the magnetised state. More negative OCP and a higher corrosion rate of magnetised NdFeB material were explained by the paramagnetism of O_2 molecules that affect oxygen transport when a magnetic field is present. An increased ion transport at the sample surface causes an increased supply of oxidising species to the magnet/electrolyte interface, contributing to the increased corrosion rate by forming a complex network of crevices.[128–130]

Improvement of corrosion resistance of sintered NdFeB magnets by the modification of the surface using protection coatings.— The progression of corrosion of sintered NdFeB magnets is mitigated by the deposition of organic polymer coatings or protective metal coatings at the surface. This is also the most common way of protecting magnets in industrial applications.

As described in the previous chapters, sintered NdFeB magnets are highly susceptible to oxidation when exposed to air and atmospheric moisture, compromising their structural integrity and leading to breakage. To prevent this process, the magnets must be coated and protected, especially in demanding environments. The surface modifications to improve corrosion resistance should not degrade the required magnetic properties. Various coating options are available for custom magnets, and their selection should be based on the specific conditions of the operating environments, particularly factors like high acidity and humidity.

The protective coatings are often applied in multiple layers to enhance durability and resistance to abrasion. There are many different commercially available coatings; some are summarised in Table VII and presented below.

Surface treatment must be the last step for sintered NdFeB permanent magnets, especially for those that should maintain high performance in humid and corrosive environments. Different types of coatings are applied using various techniques. Several chemical surface treatments can also be applied—either as standalone methods or as pretreatments—to enhance the performance of
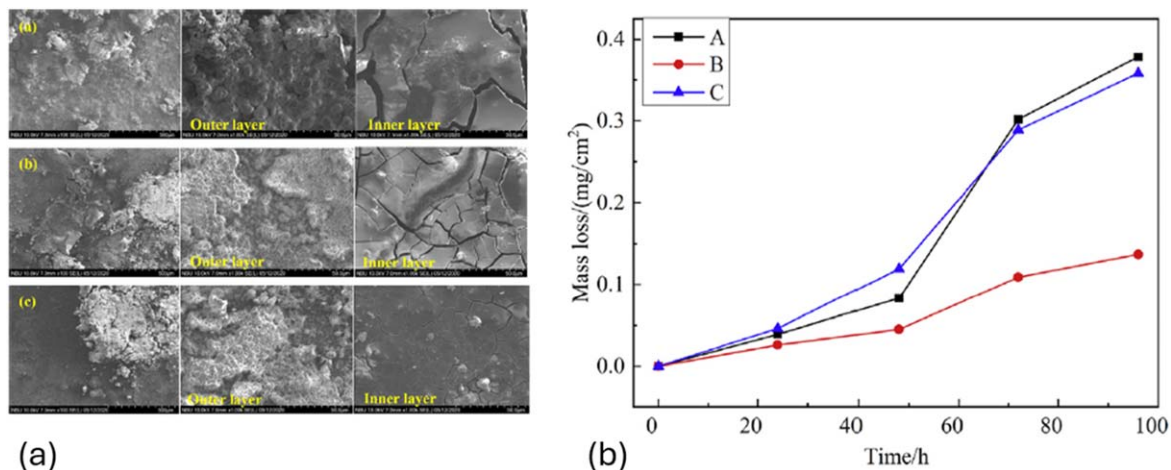
Figure 14. Some examples of the improvement of corrosion resistance of NdFeB magnets being modified by intergranular addition of (a) different Dy contents after immersion in 3.5 wt% NaCl solution for 144 h[91] and (b) mass loss for the (Ce,Pr,Nd)-Fe-B magnets with different (Pr,Nd)-Al alloy contents (A-0 wt%, B-2 wt% and C-3 wt%) in 120 °C and 100% relative humid atmosphere.[93] *Reprinted with permission from Emerald Group Publishing Limited and International Academic Publishers.*
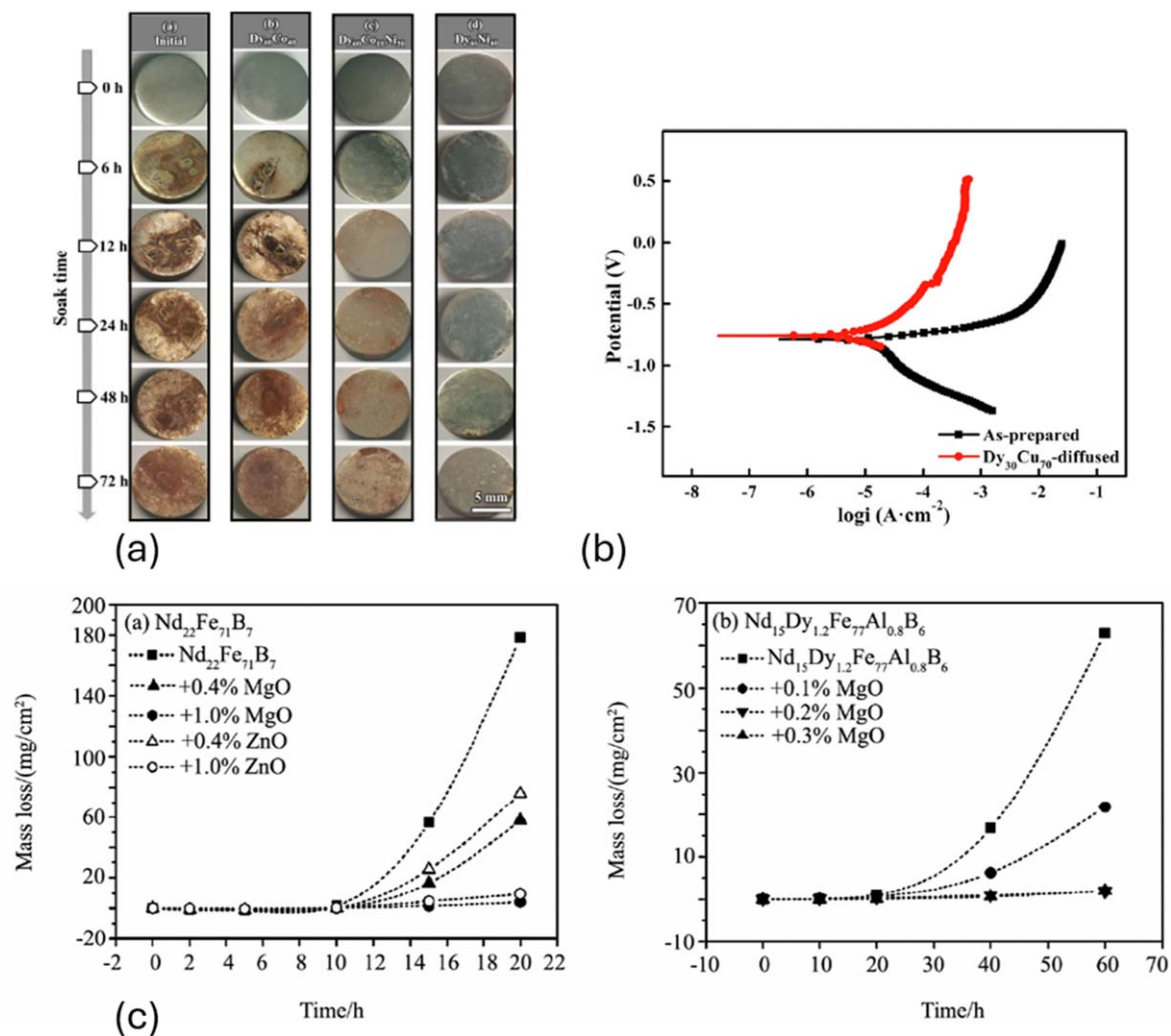
Figure 15. Some examples of the improvement of corrosion resistance of NdFeB magnets being modified by grain boundary diffusion of (a) heavy rare Earth magnets with different Ni contents diffused after soaking in 3.5 wt% NaCl solution for different times,[110] (b) the potentiodynamic polarization curves for as-prepared and DyCu-diffused magnets[101] and (c) magnets with and without MgO and ZnO addition after exposure in the autoclave.[114] *Reprinted with permission from Pergamon and Elsevier B.V.*

Table VII. Different types of commercial coatings used on sintered NdFeB magnets, with their benefits and drawbacks.

Type of commercial coating for sintered NdFeB magnets	Benefits	Drawbacks	Selected references
Nickel (Ni–Cu–Ni)	Durable, resilient against abrasion, resilient in humid environments, and with a low cost-to-performance ratio.	Resistant to acidic or saline environments.	47,131
Zinc (Zn)	Resistant against abrasion and humidity, can withstand acidic and saline environments, and has a low cost-to-performance ratio.	Degrades in salt water.	132
Gold (Ni–Cu–Ni–Au) and silver (Ni–Cu–Ni–Ag)	Similar response to Ni–Cu–Ni but more chemically inert.	High cost-to-performance ratio—very expensive last layer.	133,134
Chrome (Ni–Cu–Ni–Cr, Al–Cr)	Resilient against abrasion.	Degrades in acidic and saline environments.	135–137
Epoxy (Ni–Cu–Ni–epoxy or epoxy alone)	Resistant to corrosion, good for outdoor applications.	Lacks impact resistance, prone to abrasion/scratch, medium cost-to-performance ratio.	138,139
Teflon	Resistant to moisture/hydrophobic, resilient against abrasion.	Medium cost to performance ratio.	
Plastic or rubber, parylene	Highly corrosion resistant, Increased friction, moisture and dielectric barrier.	Medium cost-to-performance ratio, decreased magnetic pull.	140,141
Titanium nitride (TiN)	Good chemical and corrosion stability, frequently used in medical and dental applications.	High cost-to-performance ratio, not suitable for use in acidic solutions.	142–144

coatings by passivation of the surface, i.e. formation of an insoluble passivation film by reacting metal ions with anions from the solution. These chemical treatments include phosphatisation,[145–150] and conversion coatings.[151–153] The phosphate layer could also have a beneficial effect on the corrosion and adhesion of organic coatings to NdFeB magnets.[153] Phosphatization has no significant impact on magnetic properties or the dimension of magnets, as very thin layers are formed (below one μm). The passivation of the coating surface, besides phosphate passivation, also includes chromate passivation, rare Earth passivation-very often incorporating Ce,[151,154,155] and composite passivation.[156]

Silanisation[157–162] is also a surface modification technique, which involves applying silane coupling agents that chemically bond to the surface and create reactive groups (e.g., –OH, –NH$_2$, –epoxy) for further bonding with polymers or coatings. Further, sol−gel coatings[163–166] are also considered standalone protective coatings or as part of multilayer systems for corrosion resistance and adhesion promotion. Sol−gel method is a wet-chemical process where a solution (sol) gradually evolves into a gel-like network, which is then deposited and cured on a surface to form a thin, glass-like (inorganic or hybrid) coating.

Epoxy resin coatings are applied as a thin layer to encapsulate NdFeB magnets, protecting against moisture, chemicals, and mechanical damage. However, pure epoxy coating is far from reaching the requirements for anticorrosive coating of NdFeB magnets because of the defects in epoxy coating: micropores and cracks generated during curing will form a channel to accelerate the penetration of electrolyte solution and shorten the corrosion cycle of the coating.[167] In practical applications, defects in epoxy coatings allow the penetration of corrosive agents such as water, oxygen, and ions. This infiltration compromises the coating's anticorrosive effectiveness. Due to this fact, different types of fillers are added to the resins and, therefore, become composite coatings. Commonly used fillers are different nanoparticles,[139,168–173] ceramic and metal oxides[174,175] and others with targeted goals like improving barrier properties, blocking the diffusion of corrosive species, or actively inhibiting corrosion. One of the newer options for filler is also graphene.[176]

Another polymer coating is a unique type of conformal coating made from poly-para-xylylene (parylene). Parylene coatings[141,177–179] are thin, uniform, and highly protective layers applied through the chemical vapour deposition (CVD) process. Despite the higher cost and equipment requirements, their benefits in terms of protection and biocompatibility make them a valuable choice for a variety of industries. Silver/gold platings are sometimes used for NdFeB magnets in applications requiring high electrical conductivity or that are safe for biological use.[144] These coatings also have a nice decorative finish.

High-entropy alloys (HEA) or multi-principal element alloys (MEAs) are a class of metallic alloys composed of five or more principal elements in nearly equal atomic concentrations, as opposed to traditional alloys, which typically have a dominant component with small amounts of other elements added for specific properties.[180,181] This is a relatively new research area, but new ideas for using these alloys in the form of a coating to protect sintered NdFeB magnets from corrosion have already been tested. These tests show a promising improvement in the corrosion resistance of sintered NdFeB magnets by HAE coating.[182]

Titanium nitride (TiN) is a hard, ceramic-like material often used as a protective coating due to its excellent corrosion resistance, wear resistance, and chemical and metallurgical stability.[183,184] TiN is usually applied via PVD (physical vapour deposition) methods like magnetron sputtering or arc ion plating, producing a thin, uniform, and adherent layer.[142,185] Multilayers of Ti/TiN coatings offer even better anticorrosion protection.[186,187]

Tin coatings on NdFeB magnets are a less common but effective corrosion protection method, especially when combined with other coating layers or used in specialised environments.[188,189] Tin coatings offered better corrosion resistance than nickel coatings during salt spray testing. Corrosion began at coating defects as pitting, with damage severity linked to defect presence.[190]

Aluminium coatings on sintered NdFeB magnets provide an acceptable solution for corrosion protection due to the natural oxidation of aluminium and its ability to form a durable oxide layer. These coatings are typically applied through PVD,[191–199] spray coating,[200] electroplating,[201] or dip coating methods.[202] Aluminium coatings offer relatively good mechanical protection, cost-effectiveness, and minimal impact on the magnet's magnetic properties. The Al coating was envisioned as a sacrificial anode to the sintered NdFeB, but it cannot provide complete protection when an aggressive corrosive medium penetrates it, with the underlying NdFeB being prone to galvanic corrosion. Different elements have been added to improve Al coatings further. Cr plays an important role in enhancing the coating hardness and modifying the diffusion process of Al during the annealing to obtain a dense as-annealed coating with a grain boundary modification effect.[136,137,203] Manganese
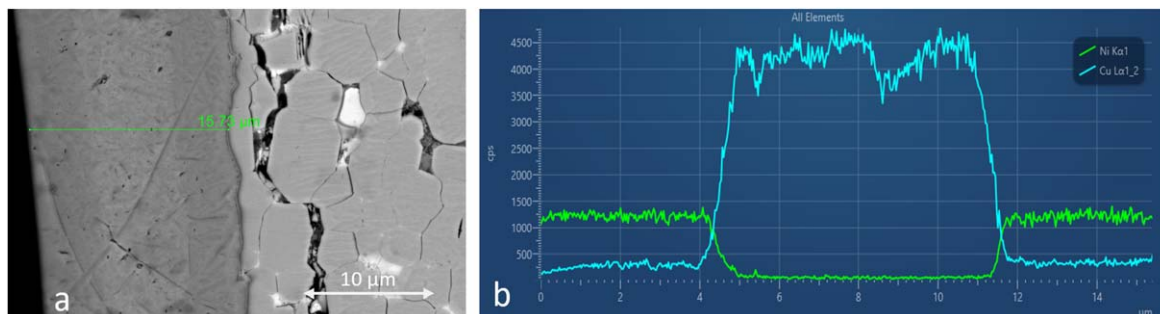
Figure 16. (a) SEM image (15 kV, back-scattered electron mode) and (b) line EDS analysis of the cross-section Ni–Cu–Ni coating on sintered NdFeB magnet (Ni-green line, Cu-blue line).

(Mn) is also added to Al to create an amorphous Al–Mn coating, which shows an anodic sacrificial protection with a low corrosion rate for NdFeB.[204,205]

Zn, as already presented for Al, is an active metal. The coating deposited using a common electrodeposition process is not dense enough and contains many pores; the untreated underlying matrix of NdFeB will react with water and oxygen in the air, thus leading to its corrosion and affecting its service lifetime. Zinc also serves as a sacrificial coating, which corrodes preferentially to the magnet, effectively shielding its surface from environmental degradation. Therefore, passivation treatment needs to be carried out on the surface of Al and Zn metal coatings.[132,206,207] To eliminate this deficiency, nonaqueous electroplating processes for coating formation have been developed and are carried out from a chloride-free nonaqueous bath.[208,209]

Nickel coatings on NdFeB magnets are one of the most common surface treatments to protect these powerful but brittle and corrosion-prone magnets. The most common application method is electroplating,[190,210] which provides a relatively uniform and adherent coating and is cost-effective, scalable and compatible with complex magnet shapes. To improve the problem of inferior adhesion[211] and poor protection performance of traditional electroplated coating on sintered NdFeB, improvements were proposed, like PVD[212–214] and CVD. Also, a multilayer metal coating can help achieve better corrosion resistance for the NdFeB magnet.[215,216] Further, combinations with other types of elements are common, like Ni–Al,[217,218] Ni–Co,[219–221] Ni–P,[222–225] Ni–Cu,[226] and most commonly used in industrial practice triple-layered Ni–Cu–Ni coating.[227]

However, when coatings are applied to sintered NdFeB magnets with an electroplating process, a traditional and mature surface treatment method widely used in actual production, hydrogen damage (or hydrogen embrittlement) can occur. This is a degradation mechanism where hydrogen atoms diffuse into a metal,[44,228] leading to cracking, blistering, or loss of mechanical integrity. During electroplating, especially in acidic baths, water reduction can occur alongside the necessary metal ion reduction.

Deposition of Ni–Cu–Ni coatings on sintered NdFeB magnets and their corrosion properties.—The triple-layered Ni–Cu–Ni layer, which consists of nickel, copper, and nickel, is widely recognised for its durability and versatility. It is used in many applications, owing to its adaptability to most environments, but it is particularly prevalent in industrial permanent magnet motors. While it is an excellent choice for indoor use, the Ni–Cu–Ni coating can also be employed outdoors, provided it is safeguarded from moisture and rainfall. Another key advantage of this coating is its robust abrasion resistance, further enhancing its durability and lifespan.

The outer nickel layer provides excellent resistance to corrosion and oxidation, and the copper middle layer acts as a barrier to prevent further penetration of moisture or corrosive agents. The inner Ni layer acts as a base coat, providing initial protection and improving adhesion for subsequent layers. Each layer smooths the defects of a previous layer, making it stronger and more resistant to environmental conditions. The typical thickness of such a three-layered Ni–Cu–Ni coating is 10–20 micrometres. Figure 16 shows the scanning electron microscopy and energy dispersion X-ray spectroscopy (SEM/EDS) analysis of the cross-section of a Ni–Cu–Ni coating deposited on a sintered NdFeB magnet.

Before applying the coating, pretreatments of the magnet surface are necessary. Usually, mechanical polishing or blasting is followed by cleaning/degreasing the specimens in an alkaline solution to remove the surface imperfections. After that, the surface is chemically treated (e.g., with acid etching) to improve the adherence of the coating layers. Finally, the surface is cleaned with deionised water and properly dried to avoid moisture trapped between the magnet material and coating. The sintered NdFeB surface is then ready to be coated.[211,229]

There are several application processes for applying Ni–Cu–Ni coatings that can be sorted into two categories. The first comprises non-electrochemical methods such as spraying, dipping, or powder coatings, commonly called "coated Ni." Alternatively, the second category includes the electrochemical process of electroplating, commonly referred to as "plated Ni."[230] Electroplating bath for applying the Ni layer is usually composed of nickel sulfate, which acts as a nickel supply, nickel chloride (enhances conductivity, ensures efficient anode dissolution), boric acid (buffers the bath, stabilising the pH near the cathode) and some other additives which improve the appearance and mechanical properties of the deposit. This formulation is commonly used in decorative and functional nickel electroplating processes, including as a base layer for multi-layer coatings (e.g., Ni–Cu–Ni plating).[231] Table VIII gathers key differences between both techniques for applying Ni (and Cu) layers.

In corrosive media, the Ni–Cu–Ni coating offers excellent protection in mild conditions (humid and weakly acidic

Table VIII. Summary of key differences between techniques for applying layers of Ni.

Feature	Coated Ni	Plated Ni
Application	Spray, dip, or other coating methods.	Electroplating process.
Layer Uniformity	May vary depending on the method.	Highly uniform.
Adhesion	Can be less strong than the plated Ni method.	Very strong due to electrochemical bonding.
Durability	Moderate to high.	Generally high.
Typical Use	Flexible and layered applications.	Precision and durability in harsh environments.

environments) and moderate resistance in saline or close to neutral, acidic environments, provided the coating is defect-free. However, additional protective measures or alternative coatings (e.g., epoxy or hybrid) may be required for prolonged exposure to harsh or highly corrosive environments.

The kinetics of high-temperature oxidation on Ni–Cu–Ni coatings was found to be temperature-dependent.[232] The oxidation product varied from CuO through NiO–Cu_2O mixed phase to NiO. The presence of the Ni–Cu–Ni coating reduces the overall oxidation rate at temperatures up to 1000 °C.

Conclusions and Future Outlook

The development of sintered NdFeB (neodymium–iron–boron) magnets is expected to continue evolving to meet the demands of modern technologies and industries. These magnets are crucial in applications requiring high energy density and compact designs, such as electric vehicles (EVs), wind turbines, robotics, and advanced electronics. Future research needs to address several key research and development areas. Ongoing research aims to improve the intrinsic properties of NdFeB, such as higher maximum energy product $((BH)_{max})$ and coercivity (H_{cj}). The development of magnets with improved resistance to high temperatures is taking place, especially for EVs and industrial motors. Another vital area of research is how to become less dependent on critical rare earth elements. Efforts focus on reducing or eliminating Dy and Tb in sintered NdFeB magnets through grain boundary engineering and advanced manufacturing techniques. Although unlikely to replace NdFeB in high-performance applications, research into alternative magnet systems (rare-earth-free alternatives) continues to ensure supply chain resilience. Recycling of sintered NdFeB magnets should gain more attention to increase the sustainability of the magnets' production. Efficient methods for recovering rare earth elements from end-of-life products are being developed.

In addition to manufacturing and recycling processes, efficient corrosion protection is essential. Past studies have explored corrosion mechanisms in different corrosive environments, and basic knowledge is available. Different protection coating materials and application techniques have been established in daily industrial practices. Contemporary production methods aimed at microstructural modifications, including intergranular addition and grain boundary diffusion using heavy and light rare earths and non-rare earth elements and compounds, have progressed to a level at which mechanical properties and coercivity are significantly improved. These modifications also improve the corrosion resistance of the NdFeB magnets. The degree of improvement depends mainly on chemical composition and processing techniques. It is noteworthy that the majority of literature studies consider electrochemical experiments as one of the properties of the overall behaviour of magnets, and more comprehensive studies are required to fully explain the mechanism of electrochemical corrosion of modified magnets. Namely, an in-depth understanding of the corrosion mechanisms in different environments will represent a more solid ground for further improvements. Further, standardised approaches are needed for a comprehensive comparison of the materials properties obtained by different production routes. The effect of magnetisation on the corrosion properties of the magnets represents another issue worth further investigation.

Considering the increasing use of sintered magnets in automobile and other industries, the knowledge of corrosion mechanisms, where magnets are in non-aqueous media, such as automatic transmission fluids, should be studied more closely. Currently, the lubrication of electric motor components in electrified vehicles is carried out mainly by automatic transmission fluids.[114,115] During vehicle operation, sintered magnets are exposed to ATF at temperatures above 130 °C. Such high temperatures may lead to the decomposition of additives and the formation of new species, which can accelerate corrosion.[233–235] The effects of automatic transmission fluid components and elevated temperature on the corrosion of

sintered magnets have not been studied in great detail. The gap in this knowledge should be overcome to ensure efficient implementation of magnets in harsh operating environments for extended periods.

The prospects of corrosion protection for sintered NdFeB magnets and their coatinigs should include advancements in materials, technologies, and processes to improve durability, environmental resistance, and cost-efficiency. The use of multilayer coatings combining different materials (e.g., nickel, copper, and epoxy) to provide synergistic protection against corrosion, mechanical wear, and environmental degradation is nowadays a standard. However, new coating materials, like graphene-based coatings, ceramic and hybrid coatings, nano-coatings, and self-healing coatings, are gaining attention. These advancements will enable the magnets to function reliably in increasingly demanding environments, supporting their expanding role in critical applications.

ORCID

Ingrid Milošev https://orcid.org/0000-0002-7633-9954

References

1. M. Sagawa, S. Fujimura, N. Togawa, H. Yamamoto, and Y. Matsuura, *J. Appl. Phys.*, **55**, 2083 (1984).
2. J. J. Croat, J. F. Herbst, R. W. Lee, and F. E. Pinkerton, *J. Appl. Phys.*, **55**, 2078 (1984).
3. S. Sugimoto, *J. Phys. D: Appl. Phys.*, **44**, 064001 (2011).
4. O. Gutfleisch, M. A. Willard, E. Brück, C. H. Chen, S. G. Sankar, and J. P. Liu, *Adv. Mater.*, **23**, 821 (2011).
5. Y. Yang et al., *J. Sustain. Metall.*, **3**, 122 (2017).
6. D. Brown, B.-M. Ma, and Z. Chen, *J. Magn. Magn. Mater.*, **248**, 432 (2002).
7. B. Jones, R. J. R. Elliott, and V. Nguyen-Tien, *Appl. Energy*, **280**, 115072 (2020).
8. J. M. D. Coey, *IEEE Trans. Magn.*, **47**, 4671 (2011).
9. J. U. Otaigbe, J. Xiao, H. Kim, and S. Constantinides, *J. Mater. Sci. Lett.*, **18**, 329 (1999).
10. P. K. Sokolowski, "Processing and protection of rare earth permanent magnet particulate for bonded magnet applications." *Master Thesis*, Iowa State University, USA (2007), http://osti.gov/servlets/purl/933032/.
11. E. A. Gorbachev, E. S. Kozlyakova, L. A. Trusov, A. E. Sleptsova, M. A. Zykin, and P. E. Kazin, *Russ. Chem. Rev.*, **90**, 1287 (2021).
12. A. Trench and J. P. Sykes, *Engineering*, **6**, 115 (2020).
13. B. Podmiljšak, B. Saje, P. Jenuš, T. Tomše, S. Kobe, K. Žužek, and S. Šturm, *Materials*, **17**, 848 (2024).
14. J. M. D. Coey, *Engineering*, **6**, 119 (2020).
15. S. Shaw and S. Constantinides, 8th International Rare Earth Conference, 13–15 November, Hong Kong (2012) chrome-extension://efaidnbmnnnibpcajpcglcle-findmkaj/https://www.magmatllc.com/PDF/Permanent%20magnets%20-%20the%20demand%20for%20rare-earths%20-%20Shaw%20and%20Constantinides%20-%202012.pdf (13-15 November 2012).
16. D. D. München and H. M. Veit, *Waste Manag.*, **61**, 372 (2017).
17. T. Crozier-Bioud, V. Momeni, J. Gonzalez-Gutierrez, C. Kukla, S. Luca, and S. Rolere, *Mater. Today Phys.*, **34**, 101082 (2023).
18. S. Dong, W. Li, H. Chen, and R. Han, *AIP Adv.*, **7**, 056237 (2017).
19. J. M. D. Coey, *Scr. Mater.*, **67**, 524 (2012).
20. R. Skomski and J. M. D. Coey, *Scr. Mater.*, **112**, 3 (2016).
21. L. Li, L. Wang, G. Yang, H. Zhang, and X. Hua, *J. Alloys Compd.*, **910**, 164951 (2022).
22. *Magnetic Material for Motor Drive Systems: Fusion Technology of Electromagnetic Fields* K. Fujisaki (ed.), (Springer, Singapore) (2019).
23. S. Liang et al., *J. Alloys Compd.*, **1003**, 175689 (2024).
24. M. Budzynski, V. C. Constantin, A.-M. J. Popescu, Z. Surowiec, T. M. Tkachenka, and K. I. Yanushkevich, *Nukleonika*, **60**, 7 (2015).
25. M. Pourbaix, *Atlas of Electrochemical Equilibria in Aqueous Solutions* (NACE and Cebelcor, Houston, TX, Brussels) (1974).
26. L. Schultz, A. M. El-Aziz, G. Barkleit, and K. Mummert, *Mater. Sci. Eng. A*, **267**, 307 (1999).
27. G. Barkleit, A. M. El-Aziz, F. Schneider, and K. Mummert, *Mater. Corros.*, **52**, 193 (2001).
28. A. A. El-Moneim, A. Gebert, M. Uhlemann, O. Gutfleisch, and L. Schultz, *Corros. Sci.*, **44**, 1857 (2002).

29. M. Rada, A. Gebert, I. Mazilu, K. Khlopkov, O. Gutfleisch, L. Schultz, and W. Rodewald, *J. Alloys Compd.*, **415**, 111 (2006).
30. I. Gurappa, *J. Alloys Compd.*, **360**, 236 (2003).
31. J. Zheng, L. Jiang, and Q. Chen, *J. Rare Earths*, **24**, 218 (2006).
32. Y. W. Song, H. Zhang, H. X. Yang, and Z. L. Song, *Mater. Corros.*, **59**, 794 (2008).
33. J. Ni, X. Cui, X. Liu, H. Cui, Z. Xue, Z. Jia, C. Wang, J. Ma, and S. Gong, *Mater. Chem. Phys.*, **162**, 518 (2015).
34. G. W. Warren, G. Gao, and Q. Li, *J. Appl. Phys.*, **70**, 6609 (1991).
35. A. Saliba-Silva, R. N. Faria, M. A. Baker, and I. Costa, *Surf. Coat. Technol.*, **185**, 321 (2004).
36. E. Isotahdon, E. Huttunen-Saarivirta, S. Heinonen, V.-T. Kuokkala, and M. Paju, *J. Alloys Compd.*, **626**, 349 (2015).
37. H. Bala, G. Pawlowska, S. Szymura, and Y. M. Rabinovich, *Br. Corros. J.*, **33**, 37 (1998).
38. L. Yang, J. Ouyang, Z.-M. Wang, and G.-L. Song, *J. Mater. Eng. Perform.*, **33**, 4740 (2023).
39. G. Yan, P. J. McGuiness, J. P. G. Farr, and I. R. Harris, *J. Alloys Compd.*, **478**, 188 (2009).
40. G. L. Yan, A. J. Williams, J. P. G. Farr, and I. R. Harris, *J. Alloy. Compd.*, **292**, 266 (1999).
41. D. F. Cygan and M. J. McNallan, *J. Magn. Magn. Mater.*, **139**, 131 (1995).
42. A. A. El-Moneim and A. Gebert, *J. Appl. Electrochem.*, **33**, 795 (2003).
43. A. A. El-Moneim, *Corros. Sci.*, **46**, 2517 (2004).
44. H. Yang, S. Mao, and Z. Song, *Mater. Corros.*, **63**, 292 (2012).
45. K. Zhang, E. Fan, J. He, X. Li, and Y. Huang, *J. Magn. Magn. Mater.*, **538**, 168309 (2021).
46. A. Popescu, J. Calderon-Moreno, K. Yanushkevish, A. Aplevich, O. Demidenko, E. Neacsu, and V. Constantin, *J. Braz. Chem. Soc.*, **35**, e–20230089 (2024).
47. K. Chitrada, K. S. Raja, B. Pesic, and I. Charit, *Electrochim. Acta*, **123**, 23 (2014).
48. E. Isotahdon, E. Huttunen-Saarivirta, V.-T. Kuokkala, and M. Paju, *Mater. Chem. Phys.*, **135**, 762 (2012).
49. R. Sueptitz, M. Uhlemann, A. Gebert, and L. Schultz, *Corros. Sci.*, **52**, 886 (2010).
50. T. Ishii, N. Tsuyuno, T. Sato, and M. Masuda, *IEEE Trans. Compon. Packaging Technol.*, **29**, 213 (2006).
51. M. A. Fazal, A. S. M. A. Haseeb, and H. H. Masjuki, *Fuel Process. Technol.*, **91**, 1308 (2010).
52. H. Jawadi, "'Corrosion Resistance of Permanent Magnets for Application in Heavy-Duty Vehicles." *Master Thesis*, Karlstad University, Sweden (2022), https://urn.kb.se/resolve?urn=urn:nbn:se:kau:diva-89322.
53. A. T. Hoang, M. Tabatabaei, and M. Aghbashlo, *Energy Sources Part A*, **42**, 2923 (2019).
54. C. I. Rocabruno-Valdés, J. A. Hernández, A. U. Juantorena, E. G. Arenas, R. Lopez-Sesenes, V. M. Salinas-Bravo, and J. G. González-Rodriguez, *Corros. Eng. Sci. Technol.*, **53**, 153 (2018).
55. F. E. Pinkerton, M. P. Balogh, N. Ellison, A. Foto, M. Sechan, M. M. Tessema, and M. P. Thompson, *J. Magn. Magn. Mater.*, **417**, 106 (2016).
56. M. Martínez Gomez, *Encyclopedia of Electrical and Electronic Power Engineering*, ed. J. García 219 (Elsevier, Oxford) (2023), https://sciencedirect.com/science/article/pii/B9780128212042001240.
57. F. Agaki, "Magnetic Domain Structures and Techniques in Micromagnetics Simulation." *Magnetic Material for Motor Drive Systems. Engineering Materials*, ed. K. Fujisaki (Springer, Singapore) (2019).
58. T. G. Woodcock, Y. Zhang, G. Hrkac, G. Ciuta, N. M. Dempsey, T. Schrefl, O. Gutfleisch, and D. Givord, *Scr. Mater.*, **67**, 536 (2012).
59. B. E. Davies, R. S. Mottram, and I. R. Harris, *Mater. Chem. Phys.*, **67**, 272 (2001).
60. Q. Zhou, W. Li, Y. Hong, L. Zhao, X. Zhong, H. Yu, L. Huang, and Z. Liu, *J. Rare Earths*, **36**, 379 (2018).
61. H. Sepehri-Amin, Y. Une, T. Ohkubo, K. Hono, and M. Sagawa, *Scr. Mater.*, **65**, 396 (2011).
62. Y. Zhang, F. Gu, Z. Su, S. Liu, C. Anderson, and T. Jiang, *Metals*, **10**, 841 (2020).
63. T. L. Chen, J. Wang, C. P. Guo, C. R. Li, Z. M. Du, G. H. Rao, and H. Y. Zhou, *Calphad*, **66**, 101627 (2019).
64. M. Zakotnik, E. Devlin, I. R. Harris, and A. J. Williams, *J. Iron & Steel Res. Int.*, **13**, 289 (2006).
65. A. Walton, H. Yi, N. A. Rowson, J. D. Speight, V. S. J. Mann, R. S. Sheridan, A. Bradshaw, I. R. Harris, and A. J. Williams, *J. Clean. Prod.*, **104**, 236 (2015).
66. R.-J. Chen, Z.-X. Wang, X. Tang, W.-Z. Yin, C.-X. Jin, J.-Y. Ju, and A.-R. Yan, *Chinese Phys. B*, **27**, 117504 (2018).
67. R. Chen, X. Xia, X. Tang, and A. Yan, *Materials*, **16**, 4789 (2023).
68. J. F. Liu, P. Vora, M. H. Walmer, E. Kottcamp, S. A. Bauser, A. Higgins, and S. Liu, *J. Appl. Phys.*, **97**, 10H101 (2005).
69. P. P. Mohapatra, G. Li, P. Alagarsamy, and X. Xu, *Mater. Futures*, **3**, 042101 (2024).
70. H. Kaneko, M. Homma, and M. Okada (ed.), *Proceedings of the 16th International Workshop on Rare-Earth Magnets and Their Applications*, Sendai, Japan (The Japan Institute of Metals) (2000).
71. K. Loewe, D. Benke, C. Kübel, T. Lienig, K. P. Skokov, and O. Gutfleisch, *Acta Mater.*, **124**, 421 (2017).
72. J. He, J. Cao, Z. Yu, W. Song, H. Yu, M. Hussain, and Z. Liu, *Metals*, **11**, 1434 (2021).
73. W. Chen, J. M. Luo, Y. W. Guan, Y. L. Huang, M. Chen, and Y. H. Hou, *J. Phys. D: Appl. Phys.*, **51**, 185001 (2018).
74. Z. Liu, J. He, Q. Zhou, Y. Huang, and Q. Jiang, *J. Mater. Sci. & Technol.*, **98**, 51 (2022).
75. M. Soderžnik, K. Ž. Rožman, S. Kobe, and P. McGuiness, *Intermetallics*, **23**, 158 (2012).
76. Z. Liu, J. He, and R. V. Ramanujan, *Mater. & Des.*, **209**, 110004 (2021).
77. F. Chen, *J. Magn. Magn. Mater.*, **514**, 167227 (2020).
78. J. He, B. Zhou, X. Liao, and Z. Liu, *J. Mater. Res. Technol.*, **28**, 2535 (2024).
79. K. Hono and H. Sepehri-Amin, *Scr. Mater.*, **154**, 277 (2018).
80. A. Kumari and S. K. Sahu, *Separ. Purif. Technol.*, **317**, 123527 (2023).
81. W. F. Li, H. Sepehri-Amin, T. Ohkubo, N. Hase, and K. Hono, *Acta Mater.*, **59**, 3061 (2011).
82. C. Burkhardt, S. van Nielen, M. Awais, F. Bartolozzi, J. Blomgren, P. Ortiz, M. B. Xicotencatl, M. Degri, S. Nayebossadri, and A. Walton, *J. Magn. Magn. Mater.*, **588**, 171475 (2023).
83. M. Kaya, *Curr. Opin. Green and Sustain. Chem.*, **46**, 100884 (2024).
84. R. Schulze and M. Buchert, *Resour. Conserv. Recycl.*, **113**, 12 (2016).
85. K. Binnemans, P. T. Jones, B. Blanpain, T. Van Gerven, Y. Yang, A. Walton, and M. Buchert, *J. Clean. Prod.*, **51**, 1 (2013).
86. Y. Ghorbani, I. M. S. K. Ilankoon, N. Dushyantha, and G. T. Nwaila, *Resour. Conserv. Recycl.*, **212**, 107966 (2025).
87. Y. Wu, Z. Gao, G. Xu, J. Liu, H. Xuan, Y. Liu, X. Yi, J. Chen, and P. Han, *Acta Metall. Sin.*, **57**, 171 (2021).
88. M. Bi, C. Xu, A. G. Wattoo, R. Bagheri, Y. Chen, S. Mao, Z. Lv, L. Yang, and Z. Song, *J. Alloys Compd.*, **703**, 232 (2017).
89. L. Yang, M. Bi, J. Jiang, X. Ding, M. Zhu, W. Li, Z. Lv, and Z. Song, *J. Magn. Magn. Mater.*, **432**, 171 (2017).
90. X.-N. Shi, M.-G. Zhu, R. Han, L.-W. Song, and W. Li, *Rare Met.*, **42**, 585 (2023).
91. J. Yang, Z. Li, H. Hao, and J. Li, *Anti-Corros. Meth. Mater.*, **71**, 789 (2024).
92. C.-C. Huang and C.-C. Mo, *Mater. Chem. Phys.*, **325**, 129648 (2024).
93. X. Wang, M. Zhu, F. Xia, M. Zhang, F. Liu, Y. Guo, L. Zhang, G. Zhang, and W. Li, *J. Rare Earths*, **39**, 979 (2021).
94. Y. L. Liu, J. Liang, Y. C. He, Y. F. Li, G. F. Wang, Q. Ma, F. Liu, Y. Zhang, and X. F. Zhang, *AIP Adv.*, **8**, 056227 (2018).
95. Y. Shao, J. Ni, Z. Wang, X. Wang, K. Xu, B. Song, Y. Xu, S. Zhou, T. Liu, and L. Luo, *J. Mater. Res. Technol.*, **33**, 4083 (2024).
96. M. Mehenni, A. Lounis, F. Ahnia, D. Miroud, A. Manseri, and M. Trari, *J. Mater. Eng. Perform.* (2024).
97. C.-C. Huang, C.-C. Mo, and S.-F. Ou, *J. Magn. Magn. Mater.*, **600**, 172166 (2024).
98. X. Li, J. Ni, Z. Wang, B. Song, C. Wang, and X. Cui, *J. Mater. Eng. Perform.*, **33**, 8954 (2024).
99. X. Zhang, Y. Ma, B. Zhang, Y. Li, M. Lei, F. Wang, M. Zhu, and X. Wang, *Corros. Sci.*, **87**, 156 (2014).
100. G. Dai, W. Yin, X. Tang, J. Ju, L. Wu, Y. Cui, R. Chen, and A. Yan, *J. Magn. Magn. Mater.*, **587**, 171321 (2023).
101. Y. L. Huang, Q. Rao, Q. Feng, Z. J. Wu, Y. F. Yao, Y. H. Hou, W. Li, and J. M. Luo, *J. Mater. Res. Technol.*, **20**, 3094 (2022).
102. T. Zhou, X. Yang, Q. Wang, J. Chen, W. Bao, B. Yu, R. Liu, and G. Xie, *J. Alloys Compd.*, **968**, 172079 (2023).
103. Z. Toujun, W. Bao, Z. Xu, M. Zhao, X. Huang, W. Wei, R. Liu, and G. Xie, *Intermetallics*, **162**, 108027 (2023).
104. X. Zhang, W. Qiu, Y. Xu, X. Liao, Q. Zhou, H. Yu, and Z. Liu, *J. Mater. Sci.: Mater. Eng.*, **20**, 7 (2025).
105. J. Yan, Q. Wu, X. Hu, J. Jia, Y. Zhao, M. Zou, and H. Ge, *J. Magn. Magn. Mater.*, **600**, 172129 (2024).
106. J. Yan, Q. Wu, H. Ge, Z. Xi, and J. Liang, *Mater. Chem. Phys.*, **315**, 128901 (2024).
107. L. Wang, W. Li, X. Wang, Z. Deng, and S. Gao, *Molecules*, **30**, 594 (2025).
108. J. Tang, W. Huang, and D. Li, *J. Rare Earths*, **42**, 1710 (2024).
109. Z. Shi, N. Shi, Y. Zhang, S. Zhang, J. Sun, V. Mandić, L. Zhao, and X. Zhang, *J. Alloys Compd.*, **1010**, 177875 (2025).
110. J. Cao, S. Chen, Z. Yu, J. He, H. Yu, Z. Xu, and Z. Liu, *Mater. Res. Bull.*, **180**, 113048 (2024).
111. M. Ji et al., *Mater. Charact.*, **223**, 114881 (2025).
112. W. Chen, Y. L. Huang, J. M. Luo, Y. H. Hou, X. J. Ge, Y. W. Guan, Z. W. Liu, Z. C. Zhong, and G. P. Wang, *J. Magn. Magn. Mater.*, **476**, 134 (2019).
113. Y. Li et al., *Chinese Phys. B*, **33**, 037508 (2024).
114. W. Mo, L. Zhang, Q. Liu, A. Shan, J. Wu, K. Matahiro, and L. Shen, *J. Rare Earths*, **26**, 268 (2008).
115. K. Zhang, Z. Yue, Y. Ma, J. He, X. Li, W. Gong, and Y. Huang, *J. Alloys Compd.*, **969**, 172391 (2023).
116. E. Wang, C. Xiao, J. He, C. Lu, M. Hussain, R. Tang, Q. Zhou, and Z. Liu, *Appl. Surf. Sci.*, **565**, 150545 (2021).
117. B. Song, X. Li, X. Wang, X. Li, Y. Song, S. Guo, and J. Ni, *J. Mater. Sci.*, **60**, 2921 (2025).
118. A. M. El-Aziz, *Mater. Corros.*, **54**, 88 (2003).
119. I. Gurappa, *Anti-Corros. Methods Mater.*, **51**, 31 (2004).
120. S. Szymura, H. Bala, Y. Rabinovich, V. Sergeev, and G. Pawlowska, *J. Magn. Magn. Mater.*, **94**, 113 (1991).
121. M. Katter, L. Zapf, R. Blank, W. Fernengel, and W. Rodewald, *IEEE Trans. Magn.*, **37**, 2474 (2001).
122. B. Grieb, C. Pithan, E. Henig, and G. Petzow, *J. Appl. Phys.*, **70**, 6354 (1991).
123. X. Shi, M. Zhu, X. Wang, S. Zhou, X. Wang, M. Zhang, and W. Li, *J. Rare Earths*, **38**, 735 (2020).
124. S. Sunada, K. Majima, Y. Akasofu, and Y. Kaneko, *J. Alloys Compd.*, **408**, 1373 (2006).
125. Y. Cao, Y. Liu, P. Zhang, G. Xu, J. Liu, J. Chen, X. Yi, and Y. Wu, *J. Rare Earths*, **39**, 1409 (2021).

126. X. T. Li, W. Q. Liu, M. Yue, X. L. Li, X. F. Yi, X. L. Huang, D. T. Zhang, and J. W. Chen, *J. Alloys Compd.*, **699**, 713 (2017).
127. A. A. El-Moneim, A. Gebert, F. Schneider, O. Gutfleisch, and L. Schultz, *Corros. Sci.*, **44**, 1097 (2002).
128. M. Moore, R. Sueptitz, A. Gebert, L. Schultz, and O. Gutfleisch, *Mater. Corros.*, **65**, 891 (2014).
129. R. Sueptitz, K. Tschulik, M. Uhlemann, M. Katter, L. Schultz, and A. Gebert, *Corros. Sci.*, **53**, 2843 (2011).
130. I. Costa, M. C. L. Oliveira, H. G. de Melo, and R. N. Faria, *J. Magn. Magn. Mater.*, **278**, 348 (2004).
131. I. Rampin, F. Bisaglia, and M. Dabalà, *J. Mater. Eng. Perform.*, **19**, 970 (2010).
132. J. Chen et al., *J. Rare Earths*, **40**, 302 (2022).
133. H. H. Man, H. C. Man, and L. K. Leung, *J. Magn. Magn. Mater.*, **152**, 40 (1996).
134. H. H. Man, H. C. Man, and L. K. Leung, *J. Magn. Magn. Mater.*, **152**, 47 (1996).
135. C. W. Cheng, H. C. Man, and F. T. Cheng, *IEEE Trans. Magn.*, **33**, 3910 (1997).
136. Z. Shi et al., *J. Magn. Magn. Mater.*, **565**, 170222 (2023).
137. J. He, X. Liao, X. Lan, W. Qiu, H. Yu, J. Zhang, W. Fan, X. Zhong, and Z. Liu, *J. Alloy. Compd.*, **870**, 159229 (2021).
138. Y. Yang, L. Yang, Y. Sun, N. Jiang, C. Guan, X. Fang, and J. Liu, *Prog. Org. Coat.*, **173**, 107180 (2022).
139. J. Liu, L. Jiang, Z. Yang, L. Wang, Z. Gao, Q. Shen, X. Fan, and H. Yang, *Coatings*, **13**, 1897 (2023).
140. Q. Liu, Z.-X. Kang, and G. Fang, *Acta Phys.-Chim. Sin.*, **29**, 821 (2013).
141. B. Ma, A. Sun, X. Gao, X. Bao, and J. Li, *J. Magn. Magn. Mater.*, **467**, 114 (2018).
142. A. Ali, A. Ahmad, and K. M. Deen, *Mater. Corros.*, **61**, 130 (2010).
143. A. Ali, A. Ahmad, and K. M. Deen, *Surf. Engin.*, **27**, 118 (2011).
144. V. Iacovacci, I. Naselli, A. R. Salgarella, F. Clemente, L. Ricotti, and C. Cipriani, *RSC Adv.*, **11**, 6766 (2021).
145. A. M. Saliba-Silva, H. G. de Melo, M. A. Baker, A. M. Brown, and I. Costa, "Characterization of Sintered NdFeB Magnets after Phosphating in Alkaline and Acidic Environments." *Advanced Powder Technology III*, ed. L. Salgado and F. A. Filho https://www.scientific.net/book/advanced-powder-technology-iii/978-3-0357-0598-0 (Trans Tech Publications Ltd., Baech, Switzerland) 54 (2003).
146. A. M. Saliba-Silva and I. Costa, *Key Eng. Mater.*, **189**, 363 (2003).
147. X. Ding, L. Xue, X. Wang, K. Ding, S. Cui, Y. Sun, and M. Li, *J. Magn. Magn. Mater.*, **416**, 247 (2016).
148. D. Xia, *Rare Metal Mat. Eng.*, **51**, 1627 (2022).
149. P. Zhang, Q. Liu, J. Huang, J. Cui, W. Sun, B. Li, and G. Xu, *J. Alloys Compd.*, **922**, 166206 (2022).
150. J. Chen, H. Yang, G. Xu, P. Zhang, J. Lv, W. Sun, B. Li, J. Huang, D. Wang, and Y. Wu, *Surf. Coat. Technol.*, **399**, 126115 (2020).
151. S. M. T. Takeuchi, D. S. Azambuja, and I. Costa, *Surf. Coat. Technol.*, **201**, 3670 (2006).
152. Q. Li, H. Gao, J. P. Wang, and S. Y. Zhang, *Trans. Inst. Metal Finish.*, **87**, 38 (2009).
153. P. Zhang, Q. Liu, J. Huang, J. Cui, W. Sun, B. Li, and G. Xu, *J. Alloy. Compd.*, **922**, 166206 (2022).
154. K. A. Yasakau, M. L. Zheludkevich, S. V. Lamaka, and M. G. S. Ferreira, *J. Phys. Chem. B*, **110**, 5515 (2006).
155. H. Nan, L. Zhu, H. Liu, and W. Li, *Appl. Surf. Sci.*, **355**, 1215 (2015).
156. Y. Yin, H. Zhao, M. Prabhakar, and M. Rohwerder, *Corros. Sci.*, **200**, 110252 (2022).
157. J.-M. Hu, X.-L. Liu, J.-Q. Zhang, and C.-N. Cao, *Prog. Org. Coat.*, **55**, 388 (2006).
158. F. Fabiano, L. Calabrese, A. Capri, M. Curro, C. Borsellino, L. Bonaccorsi, V. Fabiano, R. Ientile, and E. Proverbio, *Sci. Adv. Mater.*, **9**, 1141 (2017).
159. W. Ju, L. Jiang, Y. Liang, S. Xu, K. Wang, Y. Yang, B. Zhu, G. Wei, and Z. Zhang, *Trans. Nonferrous Met. Soc.China*, **34**, 2928 (2024).
160. Z. Tao, L. Jiang, W. Ju, Y. Liang, Y. Yang, G. Wei, Y. Chen, and Z. Zhang, *Arab. J. Chem.*, **18**, 106057 (2025).
161. Y. Liang, L. Jiang, W. Ju, S. Xu, Z. Tao, K. Wang, Y. Yang, B. Zhu, and G. Wei, *Mater. Today Commun.*, **38**, 108319 (2024).
162. X. Ding, J. Li, M. Li, S. Ge, X. Wang, K. Ding, S. Cui, and Y. Sun, *Surf. Rev. Lett.*, **21**, 1450077 (2014).
163. M. Bragaglia, L. Paleari, L. Fazi, V. Scacco, and F. Nanni, *J. Sol-Gel Sci. Technol.*, **106**, 95 (2023).
164. F. Liu, Q. Li, L. Q. Li, S. Y. Wang, and H. X. Zhang, *Trans. Inst. Metal Finish.*, **90**, 203 (2012).
165. R. Cao, L. Zhu, H. Liu, and W. Li, *Surf. Coat. Technol.*, **309**, 820 (2017).
166. S. N. B. Hodgson, C. G. Hoggarth, H. A. Davies, and R. A. Buckley, *J. Mater. Process. Technol.*, **93**, 518 (1999).
167. M. Zhang, X. Zhao, H. Jia, H. Xing, H. Zhang, X. Wang, and C. Liu, *J. Coat. Technol. Res.*, **19**, 1409 (2022).
168. H. Yang, L. Duan, P. Zhang, G. Xu, J. Cui, J. Lv, W. Sun, B. Li, D. Wang, and J. Wu, *J. Coat. Technol. Res.*, **19**, 1317 (2022).
169. J. L. Xu, Z. X. Huang, J. M. Luo, and Z. C. Zhong, *J. Magn. Magn. Mater.*, **355**, 31 (2014).
170. J. L. Xu, Z. C. Zhong, Z. X. Huang, and J. M. Luo, *J. Alloy. Compd.*, **570**, 28 (2013).
171. Z. Shen, H. Yang, P. Zhang, J. Cui, D. Wang, W. Shen, G. Xu, and J. Lv, *J. Coat. Technol. Res.*, **21**, 1677 (2024).
172. Z.-C. Zhong, J.-L. Xu, Z.-X. Huang, and J.-M. Luo, *Rare Met.*, **33**, 703 (2014).
173. L. Shen, M. Fan, K. Zhao, M. Qiu, and Z. Tian, *Mater. Res. Express*, **5**, 086401 (2018).

174. Y. Yang, N. Jiang, Y. Sun, L. Yang, C. Guan, E. Zhang, X. Fang, and J. Liu, *J. Mater. Eng. Perform.*, **32**, 5475 (2023).
175. Z. H. Rao, J. L. Xu, J. Huang, X. H. Zhang, Y. C. Ma, and J. M. Luo, *Ceram. Int.*, **51**, 5695 (2025).
176. Y. Zou, Y. Lu, S. U. Rehman, X. Zhang, S. Luo, C. Jin, Z. Zou, B. Yang, and M. Yang, *Surf. Innov.*, **11**, 442 (2023).
177. A. Kaidarova, M. A. Khan, S. Amara, N. R. Geraldi, M. A. Karimi, A. Shamim, R. P. Wilson, C. M. Duarte, and J. Kosel, *Adv. Eng. Mater.*, **20**, 1800229 (2018).
178. V. Zablotskii, A. Dejneka, S. Kubinova, D. Le-Roy, F. Dumas-Bouchiat, D. Givord, N. M. Dempsey, and E. Sykova, *PLoS One*, **8**, e70416 (2013).
179. N. Jackson, F. J. Pedrosa, A. Bollero, A. Mathewson, and O. Z. Olszewski, *J. Microelectromech. Syst.*, **25**, 716 (2016).
180. D. B. Miracle and O. N. Senkov, *Acta Mater.*, **122**, 448 (2017).
181. S. A. Krishna, N. Noble, N. Radhika, and B. Saleh, *J. Manuf. Process.*, **109**, 583 (2024).
182. L. W. Zhang, J. L. Xu, J. Chen, J. Huang, and J. M. Luo, *J. Magn. Magn. Mater.*, **551**, 169136 (2022).
183. K. Bordji, J. Y. Jouzeau, D. Mainard, E. Payan, P. Netter, K. T. Rie, T. Stucky, and M. Hage-Ali, *Biomaterials*, **17**, 929 (1996).
184. C.-T. Kao, S.-J. Ding, Y.-C. Chen, and T.-H. Huang, *J. Biomed. Mater. Res.*, **63**, 786 (2002).
185. J. L. Li, S. D. Mao, Z. L. Song, and Q. J. Xue, *Adv. Mater. Res.*, **482–484**, 1130 (2012).
186. P. Xie, P. Wang, W. Deng, Y. Duan, Y. Chen, and Y. Huang, *J. New Mat. Electrochem. Syst.*, **23**, 20 (2020).
187. Y. Cheng, X. Pang, K. Gao, H. Yang, and A. A. Volinsky, *Thin Solid Films*, **550**, 428 (2014).
188. T. Zhang, Z. Yuan, R. Wang, B. Ma, L. Mei, and H. Zhao, *Physica B: Condensed Matter*, **636**, 413886 (2022).
189. Z. Hu, *Anti-Corros. Methods. Mater.*, **68**, 340 (2021).
190. E. Isotahdon, E. Huttunen-Saarivirta, V.-T. Kuokkala, M. Paju, and L. Frisk, *J. Alloys Compd.*, **585**, 203 (2014).
191. P. Zhang, J. Liu, G. Xu, X. Yi, J. Chen, and Y. Wu, *Surf. Coat. Technol.*, **282**, 86 (2015).
192. S. Mao, H. Yang, F. Huang, T. Xie, and Z. Song, *Appl. Surf. Sci.*, **257**, 3980 (2011).
193. S. Mao, H. Yang, Z. Song, J. Li, H. Ying, and K. Sun, *Corros. Sci.*, **53**, 1887 (2011).
194. S. Mao, H. Yang, J. Li, F. Huang, and Z. Song, *Appl. Surf. Sci.*, **257**, 5581 (2011).
195. Y. Gao, Y. Bai, H. Zhu, W. Liang, Q. Liu, H. Dong, R. Jia, and W. Ma, *J. Therm. Spray Technol.*, **30**, 2117 (2021).
196. E. Chen, K. Peng, W. Yang, J. Zhu, D. Li, and L. Zhou, *Trans. Nonferrous Met. Soc. China*, **24**, 2864 (2014).
197. Y. Cao, P. Zhang, W. Sun, W. Zhang, H. Wei, J. Wang, B. Li, X. Yi, G. Xu, and Y. Wu, *J. Rare Earths*, **39**, 703 (2021).
198. Z. Cao, X. Ding, R. Bagheri, A. G. Wattoo, C. Xu, L. Yang, L. Song, Y. Wen, and Z. Song, *Vacuum*, **142**, 37 (2017).
199. S. Mao, H. Yang, J. Li, H. Ying, and Z. Song, *Vacuum*, **85**, 772 (2011).
200. C. Ma, X. Liu, and C. Zhou, *J. Therm. Spray Technol.*, **23**, 456 (2014).
201. F. Xu, L. Jiang, J. Wu, X. Shen, Q. Huang, Y. Yu, C. Cao, G. Wei, and H. Ge, *Int. J. Electrochem. Sci.*, **12**, 517 (2017).
202. C. D. Qin, A. S. K. Li, and D. H. L. Ng, *J. Appl. Phys.*, **79**, 4854 (1996).
203. J. Zheng, M. Lin, and Q. Xia, *J. Magn. Magn. Mater.*, **324**, 3966 (2012).
204. J. Ding, B. Xu, and G. Ling, *Appl. Surf. Sci.*, **305**, 309 (2014).
205. J. Chen, B. Xu, and G. Ling, *Mater. Chem. Phys.*, **134**, 1067 (2012).
206. L. Duan, J. Chen, P. Zhang, G. Xu, J. Lv, D. Wang, W. Shen, and Y. Wu, *J. Alloy. Compd.*, **936**, 168292 (2023).
207. B. Li, X. Zhou, X. Chen, S. Fu, X. Wang, and D. Zhao, *Materials*, **15**, 7523 (2022).
208. Y. Hu, M. Aindow, I. P. Jones, and I. R. Harris, *J. Alloy. Compd.*, **351**, 299 (2003).
209. L. Xiaoya, M. Yongcun, P. Shusen, and T. Lixi, *RSC Adv.*, **14**, 8641 (2024).
210. Q. Li, X. Yang, L. Zhang, J. Wang, and B. Chen, *J. Alloy. Compd.*, **482**, 339 (2009).
211. Y. X. Heng, D. Yong, and I. S. Zhen, *J. Phys. Conf. Ser.*, **266**, 012053 (2011).
212. S. Hu, K. Peng, E. Chen, and H. Chen, *J. Mater. Eng. Perform.*, **24**, 4985 (2015).
213. Y. Lu, S. Luo, Z. Ren, Y. Zou, S. Zhong, Y. Wu, C. Liu, and M. Yang, *Surf. Coat. Technol.*, **409**, 126833 (2021).
214. L. Shen, C. Wang, Z. Tian, W. Jiang, W. Zhuo, and K. Zhao, *Int. J. Electrochem. Sci.*, **13**, 1831 (2018).
215. L. Shen, Y. Wang, W. Jiang, X. Liu, C. Wang, and Z. Tian, *Corros. Eng. Sci. Technol.*, **52**, 311 (2017).
216. M. Fan, L. Shen, M. Qiu, Z. Wang, and Z. Tian, *Int. J. Electrochem. Sci.*, **13**, 7532 (2018).
217. H. Zhang, Y. W. Song, and Z. L. Song, *Mater. Corros.*, **59**, 324 (2008).
218. N. C. Ku, C. D. Qin, and D. H. L. Ng, *IEEE Trans. Magn.*, **33**, 3913 (1997).
219. X. Yang, Q. Li, S. Zhang, H. Gao, F. Luo, and Y. Dai, *J. Solid State Electrochem.*, **14**, 1601 (2010).
220. C. Tan, Q. Li, Z. She, F. Liu, Z. Wang, and L. Li, *Mater. Sci. Technol.*, **32**, 446 (2016).
221. W. Jiang, L. Shen, M. Xu, Z. Wang, and Z. Tian, *J. Alloy. Compd.*, **791**, 847 (2019).
222. C. B. Ma, F. H. Cao, Z. Zhang, and J. Q. Zhang, *Appl. Surf. Sci.*, **253**, 2251 (2006).
223. Y. Wang, Y. Deng, Y. Ma, and F. Gao, *Surf. Coat. Technol.*, **206**, 1203 (2011).
224. L. Li, X. Cheng, and F. S. Yin, *Adv. Mater. Res.*, **535**, 1275 (2012).
225. Z. Chen, A. Ng, J. Z. Yi, and X. F. Chen, *J. Magn. Magn. Mater.*, **302**, 216 (2006).

226. J. Long, X. Xie, Y. Cai, S. Zhong, S. Luo, W. Zhang, and M. Yang, *Surf. Innov.*, **12**, 481 (2024).
227. X. Xie, Y. Cai, S. U. Rehman, I. Bulyk, S. Zhou, S. Xiong, H. Wang, B. Yang, and M. Yang, *Electrochim. Acta*, **523**, 145897 (2025).
228. A. S. Kim, F. E. Camp, and T. Lizzi, *J. Appl.Phys.*, **79**, 4840 (1996).
229. E. Isotahdon, "Corrosion losses, mechanisms and protection strategies for sintered Nd-Fe-B magnets." *PhD thesis*, Tampere University of Technology, Finland (2017).
230. C. W. Cheng, F. T. Cheng, and H. C. Man, *J. Appl. Phys.*, **83**, 6417 (1998).
231. Q. Li, H. Gao, J. P. Wang, and B. Chen, *Trans. Inst. Metal Finish.*, **87**, 149 (2009).
232. D. C. Nababan, R. Mukhlis, Y. Durandet, M. I. Pownceby, L. Prentice, and M. A. Rhamdhani, *Corros. Sci.*, **189**, 109560 (2021).
233. I. Khan, S. Ruzimov, N. Amati, and A. Tonoli, *Energies*, **15**, 945 (2022).
234. B. McCoy, *TLT*, **77**, 38 (2021).
235. E. Rodríguez, N. Rivera, A. Fernández-González, T. Pérez, R. González, and A. H. Battez, *Tribol. Int.*, **171**, 107544 (2022).